

NASA TECHNICAL
MEMORANDUM



NASA TM X-2454

NASA TM X-2454

DO NOT EXPOSE
TO SUNLIGHT

DECLASSIFIED
BY AUTHORITY OF NASA CLASSIFICATION
CHANGE NOTICE NO. 244, 12/20/72
ITEM NO. 12

WIND-TUNNEL INVESTIGATION OF EFFECTS
OF REAR UPPER SURFACE MODIFICATION
ON AN NASA SUPERCRITICAL AIRFOIL -

by Charles D. Harris and James A. Blackwell, Jr.

Langley Research Center
Hampton, Va. 23365

NATIONAL AERONAUTICS AND SPACE ADMINISTRATION - WASHINGTON, D. C. - JANUARY 1972

CONFIDENTIAL
CONFIDENTIAL

CONFIDENTIAL

1. Report No. NASA TM X-2454	2. Government Accession No.	3. Recipient's Catalog No.
4. Title and Subtitle WIND-TUNNEL INVESTIGATION OF EFFECTS OF REAR UPPER SURFACE MODIFICATION ON AN NASA SUPERCRITICAL AIRFOIL (U)		5. Report Date January 1972
7. Author(s) Charles D. Harris and James A. Blackwell, Jr.		6. Performing Organization Code
9. Performing Organization Name and Address NASA Langley Research Center Hampton, Va. 23365		8. Performing Organization Report No. L-7983
		10. Work Unit No. 742-73-01-14
		11. Contract or Grant No.
		13. Type of Report and Period Covered Technical Memorandum
12. Sponsoring Agency Name and Address National Aeronautics and Space Administration Washington, D.C. 20546		14. Sponsoring Agency Code
15. Supplementary Notes		
16. Abstract <p>Wind-tunnel tests have been conducted at Mach numbers from 0.60 to 0.81 to examine the effects on an NASA supercritical airfoil of modifying the rear upper surface to reduce the magnitude of an intermediate off-design second velocity peak. The modification was accomplished by increasing the upper surface curvature around the 50-percent-chord station and reducing the curvature over approximately the rearmost 30 percent of the airfoil while maintaining the same trailing-edge thickness.</p>		

CLASSIFICATION CHANGE

To UNCLASSIFIED By authority of NASA Langley Date 77-163
Changed by 02/19/76 Date 6/11/76
Classified Document Master Control Station, NASA
Scientific and Technical Information ~~CLASSIFIED BY 100254(10/3/76) NASA-2431~~
~~SUBJECT TO GENERAL DECLASSIFICATION~~
~~SCHEDULE OF EXECUTIVE ORDER 11652.~~
~~AUTOMATICALLY DOWNGRADED AT~~
~~TWO-YEAR INTERVALS.~~
~~DECLASSIFIED ON DECEMBER 31, 1978~~

17. Key Words (Suggested by Author(s)) Supercritical airfoils Transonic aerodynamics	
19. Security Classif. (of this report) <u>Confidential</u>	20.
GROUP 4 Downgraded every year intervals; Declassified after 12 years	

~~SECRET~~

WIND-TUNNEL INVESTIGATION OF EFFECTS OF
REAR UPPER SURFACE MODIFICATION ON
AN NASA SUPERCRITICAL AIRFOIL*

By Charles D. Harris and James A. Blackwell, Jr.
Langley Research Center

SUMMARY

An investigation has been conducted in the Langley 8-foot transonic pressure tunnel at Mach numbers from 0.60 to 0.81 to examine the effects on an NASA supercritical airfoil of modifying the rear upper surface to reduce the magnitude of an inherent intermediate off-design second velocity peak on the upper surface. The modification was accomplished by increasing the upper surface curvature around the 50-percent-chord station and reducing the curvature over approximately the rearmost 30 percent of the airfoil while maintaining the same trailing-edge thickness.

Results indicate that attempts to reduce the magnitude of the second peak in the manner described herein would have an adverse effect on drag at design conditions and suggest that the magnitude of the second peak should be less than that of the leading-edge peak.

INTRODUCTION

Considerable effort is presently being directed toward designing practical two-dimensional airfoils with good performance characteristics at supercritical speeds while retaining acceptable subcritical characteristics. Much of the recent work has centered on the newly evolved NASA supercritical airfoil of references 1 to 4. This unique airfoil, shaped to reduce the drag associated with energy losses due to shock waves and flow separation, is characterized by a large leading-edge radius, flattened upper surface, and highly cambered trailing edge.

The rear upper surface of the supercritical airfoil is shaped to accelerate the flow following the shock wave in order to produce a near-sonic plateau at design conditions. This plateau, an essential and distinctive feature of the supercritical airfoil concept, permits the boundary layer to stabilize before going through its final compression at the

~~SECRET~~
* Unpublished.

~~CONFIDENTIAL~~

trailing edge and also prevents decelerating disturbances from propagating forward and strengthening the shock wave (ref. 1). Near the design normal-force coefficient, at intermediate supercritical conditions between the onset of supersonic flow and the design point, the upper surface shock wave moves forward and the rear upper surface contour necessary to produce the near-sonic plateau at design conditions causes the flow to expand into a second region of supercritical flow in the vicinity of the three-quarter-chord station. Care must be exercised that this second region of supercritical flow is not permitted to expand to such an extent that a second shock wave is formed which would tend to separate the flow over the rear portion of the airfoil.

As part of the systematic wind-tunnel development program for the supercritical airfoil, changes in the curvature over the rear upper surface of a supercritical airfoil model were made to evaluate the effect of the magnitude of the off-design second velocity peak on the design point. The purpose of this paper is to present the results of such an evaluation, conducted in the Langley 8-foot transonic pressure tunnel over a Mach number range from 0.60 to 0.81.

SYMBOLS

Values are given in both SI and U.S. Customary Units. The measurements and calculations were made in U.S. Customary Units.

C_p pressure coefficient, $\frac{p_l - p_\infty}{q_\infty}$

$C_{p,sonic}$ pressure coefficient corresponding to local Mach number of 1.0

c chord of airfoil, centimeters (inches)

c_d section drag coefficient, $\sum c_d' \frac{\Delta z}{c}$

c_d' point drag coefficient (ref. 5)

c_m section pitching-moment coefficient about the quarter-chord point,

$$\sum_{l.s.} C_p \frac{\Delta x}{c} \left(0.25 - \frac{x}{c}\right) - \sum_{u.s.} C_p \frac{\Delta x}{c} \left(0.25 - \frac{x}{c}\right)$$

c_n	section normal-force coefficient, $\sum_{l.s.} C_p \frac{\Delta x}{c} - \sum_{u.s.} C_p \frac{\Delta x}{c}$
M	Mach number
m	slope of airfoil surface, dy/dx
p	static pressure, newtons per meter ² (pounds per foot ²)
Δp_t	total-pressure loss, newtons per meter ² (pounds per foot ²)
q	dynamic pressure, newtons per meter ² (pounds per foot ²)
R	Reynolds number based on airfoil chord
x	ordinate along airfoil reference line measured from airfoil leading edge, centimeters (inches)
y	ordinate normal to airfoil reference line, centimeters (inches)
z	vertical distance in wake profile measured from top of rake, centimeters (inches)
α	angle of attack of airfoil reference line, degrees

Subscripts:

l	local point on airfoil
∞	undisturbed stream

Abbreviations:

l.s.	airfoil lower surface
u.s.	airfoil upper surface

~~CONFIDENTIAL~~

APPARATUS AND TECHNIQUES

Much of the apparatus and many of the testing techniques used during this investigation were similar or identical to those described in references 1 and 4. The descriptions, when applicable, are repeated herein for convenience.

Wind Tunnel

The investigation was conducted in the Langley 8-foot transonic pressure tunnel. This tunnel is a single-return, rectangular wind tunnel with controls that allow for the independent variation of Mach number, stagnation pressure, temperature, and dewpoint (ref. 6). The upper and lower test-section walls are axially slotted to permit testing through the transonic speed range without the usual effects of choking and blockage. The total slot width at the position of the model averaged about 5 percent of the width of the upper and lower walls.

The solid side walls and slotted upper and lower walls make this tunnel well suited to the investigation of two-dimensional models since the side walls act as end plates while the slots permit development of the flow field in the vertical direction.

Model

Detailed discussions of the supercritical airfoil concept and design philosophy may be found in references 1 and 4 and are not repeated herein. The design conditions for the airfoils described herein were $c_n = 0.7$ at $M = 0.79$. The normal-force coefficient of 0.7 was chosen as the design goal since, when account is taken of the sweep effect, it is representative of lift coefficients at which advanced technology transports utilizing the supercritical airfoil concept are expected to cruise.

Two supercritical airfoils, each having a maximum thickness of 11 percent of the chord and a trailing-edge thickness of 1 percent of the chord, were used in this investigation. The trailing-edge thickness of the two airfoils was somewhat greater than that shown to be desirable in reference 4 but this should not affect conclusions drawn from the data presented in the present report. The models were constructed with metal leading and trailing edges and with a metal core around which plastic fill was used to form the upper and lower surfaces.

Airfoil number designations used are those assigned as part of the numbering system for the overall supercritical airfoil development program. Airfoil 5, considered to be the basic airfoil for this investigation, was derived from an earlier airfoil with a thin trailing edge (airfoil 4) by rotating the rear lower surface downward about the 64-percent-chord line to the desired trailing-edge thickness. (Airfoils 4 and 5 are compared and

~~CONFIDENTIAL~~

discussed in reference 4.) Surface slopes over the rear upper surface of airfoil 5 were modified as shown in figure 1 and the resultant airfoil designated as airfoil 6. The modification was accomplished by removing material over approximately the rear 60 percent of the upper surface without changing the trailing-edge thickness and resulted in an increase in surface curvature around the 50-percent chordwise station and a decrease in surface curvature over approximately the rearmost 30 percent of the airfoil. (For small values of slope, curvature may be approximated by dm/dx , which is the second derivative of the airfoil contour d^2y/dx^2 .) Coordinates and surface slopes for both airfoils are given in tables I and II.

The airfoil models were mounted in an inverted position and completely spanned the width of the tunnel. Angle of attack was changed manually by rotating the model about pivots in the tunnel sidewalls. Sketches of an airfoil and the profile drag rake are presented in figure 2 and a photograph of the airfoil and profile drag rake mounted in the tunnel is shown as figure 3.

Boundary-Layer Transition

Based on techniques discussed in reference 7, transition strips were applied along the 28-percent-chord line on both the upper and lower surfaces in an attempt to simulate full-scale Reynolds number boundary-layer characteristics at the trailing edge and full-scale shock-wave locations. The simulation is limited on the upper surface to those conditions in which the shock wave occurs behind the transition, that is, to the higher test Mach numbers. Full-scale simulation on the lower surface would be valid through the Mach number range of the investigation since laminar flow can be maintained ahead of the trip for all conditions. Simulated full-scale Reynolds numbers were as shown in figure 4. The transition strips consisted of 0.25-cm-wide (0.10 in.) bands of No. 90 carborundum grains.

Caution should be exercised when comparing the present results with results from earlier supercritical airfoil investigations since transition grit size and location used during earlier phases of the supercritical airfoil development program differed from that just described.

Measurements

Surface pressure measurements. - Normal forces and pitching moments acting on the airfoils were determined from surface pressure measurements. The surface pressures were obtained from flush orifices located in a chordwise row at a spanwise station $0.28c$ from the tunnel center line using differential pressure-scanning valves. The maximum range of the transducers in the valves was $\pm 68.9 \text{ kN/m}^2$ (10 lb/in^2). The orifices

were more concentrated near the leading and trailing edges of the airfoils to define the severe pressure gradients in these regions.

Wake measurements. - Drag forces acting on the airfoils, as measured by the momentum deficiency within the wake, were derived from vertical variations of the total and static pressures measured across the wake with the profile drag rake shown in figure 2(b). The rake was positioned in the vertical center-line plane of the tunnel approximately 1 chord length rearward of the trailing edge of the airfoil. The total-pressure tubes were flattened horizontally and closely spaced vertically (0.36 percent of the airfoil chord) in the region of the wake associated with skin-friction boundary-layer losses. Outside this region, the tube vertical spacing progressively widened until, in the region above the wing where only shock losses were anticipated, the total-pressure tubes were spaced approximately 7.3 percent of the chord apart. Static-pressure tubes were distributed as shown in figure 2(b). The rake was attached to the conventional center-line sting mount of the tunnel which permitted it to be moved vertically to center the close concentration of tubes on the boundary-layer wake.

Total and static pressures across the wake were also measured with the use of differential pressure scanning valves. The maximum range of the transducer in the valve connected to total pressure tubes intended to measure boundary-layer losses was $\pm 34.5 \text{ kN/m}^2$ (5 lb/in 2); the corresponding maximum range for measuring shock losses and static pressure was $\pm 6.9 \text{ kN/m}^2$ (1 lb/in 2).

Reduction of Data and Corrections

Calculation of c_n and c_m . - Section normal-force and pitching-moment coefficients were obtained by numerical integration (based on the trapezoidal method) of the local surface pressure coefficient measured at each orifice multiplied by an appropriate weighting factor (incremental area).

Calculation of c_d . - To obtain section drag coefficients from the total and static pressures behind the model, point drag coefficients for each of the total pressure measurements were computed by using the procedure of reference 5. These point drag values were then summed by numerical integration across the wake, again based on the trapezoidal method.

Corrections for wind-tunnel-wall effects. - The major interference effect of the wind-tunnel walls was an upflow at the inverted model. This upflow, proportional to the normal-force coefficient, results in the measured geometric angle of attack being significantly greater than the aerodynamic angle of attack at the higher normal-force coefficients with an attendant reduction in the slope of the curve for normal-force coefficient as a function of angle of attack. The mean value of this upflow at the midchord of the

model, in degrees, may be estimated by the theory of reference 8 to be approximately three times the section normal-force coefficient. However, based on experience in other two-dimensional tests in the 8-foot transonic pressure tunnel, such a correction is believed to be unrealistically large. Because of this uncertainty, the uncorrected geometric angles of attack are used in the results presented herein.

The theory of reference 8 also indicates that tunnel-wall blockage effects would be small; consequently, no corrections have been applied to the data to account for blockage effects.

TEST CONDITIONS

Tests were conducted at Mach numbers from 0.60 to 0.81 for a stagnation pressure of 0.1013 MN/m^2 (1 atm) with resultant wind-tunnel Reynolds numbers based on the airfoil chord as shown in figure 4. The stagnation temperature of the tunnel air was automatically controlled at approximately 322 K (120° F) and the air was dried until the dewpoint temperature in the test section was reduced sufficiently to avoid condensation effects.

PRESENTATION OF RESULTS

Comparisons of the aerodynamic characteristics of the basic airfoil 5 and the modified airfoil 6 are presented in figure 5 and the drag-rise characteristics at the design normal-force coefficient of 0.7 are summarized in figure 6. Chordwise pressure profiles are compared in figure 7 and representative wake profiles shown in figure 8. In several instances, drag data are not presented in figure 5 for the higher angles of attack because momentum losses in the wake exceeded the measuring capability of the profile drag rake.

DISCUSSION

The rear upper surface modification produced the expected reductions in the magnitude of the off-design second velocity peaks (fig. 7) with corresponding reductions in the drag at the lower normal-force coefficients (fig. 5). There was, however, a significant 6 count increase in drag coefficient (c_d increment of 0.0006 shown in fig. 6) at the design conditions ($M = 0.79$ and $c_n = 0.70$) due to the more severe buildup of boundary layer and wave losses for the modified airfoil (airfoil 6).

The key to the adverse effects of the rear upper surface modification at design conditions may be seen in the airfoil pressure and wake profiles for $M = 0.79$ and $\alpha = 1.0^{\circ}$ (figs. 7(r) and 8, respectively) which are very close to design conditions. The

combination of increased surface curvature around approximately the 50-percent chord-wise station and decreased curvature over the rearmost 30 percent of the upper surface (fig. 1) results in the flow entering the shock wave at higher local Mach numbers causing a stronger, more abrupt, shock wave on the modified airfoil.

As discussed in the Introduction, a supercritical airfoil optimized for a given design point has an inherent second velocity peak on the upper surface at intermediate off-design conditions. If allowed to expand too much, a second shock wave may be formed resulting in drag penalties at these off-design conditions. In order to establish some upper limit on the magnitude to which this second velocity peak may be permitted to expand, attention is called to the pressure profiles for angles of attack of 0.5° and 1.0° at the intermediate Mach number of 0.78 shown in figures 7(m) and 7(n) and the corresponding integrated drag data in figure 5(f). At $\alpha = 1.0^\circ$ (fig. 7(n)), which is very close to the angle of attack at which the design normal-force coefficient occurs, the magnitude of the second peak on both airfoils is less than that of the leading-edge peak. The drag levels of the two airfoils are practically the same (fig. 5(f)). At the slightly further off-design condition of $\alpha = 0.5^\circ$ (fig. 7(m)), the magnitude of the second velocity peak of airfoil 5 is on the order of that of the leading-edge peak, and the drag level of airfoil 5 is higher than that of airfoil 6 (fig. 5(f)).

Consideration of the evidence shown in these figures suggests that in order to avoid drag penalties associated with a second shock system on the upper surface at intermediate off-design conditions, a reasonable criterion would be that the magnitude of the second velocity peak should be less than that of the leading-edge peak. Further support of this criterion is provided by the pressure profiles for $M = 0.79$ and $\alpha = 0.5^\circ$ (fig. 7(q)) where the magnitude of the second peak on both airfoils exceeds the magnitudes of the leading-edge peaks, and the corresponding drag levels (fig. 5(g)) of both airfoils are slightly higher than those at adjacent angles of attack.

CONCLUDING REMARKS

A second upper surface velocity peak in the vicinity of the three-quarter-chord station at intermediate off-design conditions is inherent in the NASA supercritical airfoil concept. An investigation has been conducted in the Langley 8-foot transonic pressure tunnel at Mach numbers from 0.60 to 0.81 to examine the effects of modifying the rear upper surface of the airfoil to reduce the magnitude of this second velocity peak.

The results show that attempts to reduce the magnitude of this second velocity peak at intermediate off-design conditions in the manner described herein would have an adverse effect on drag at design conditions. Also, the results suggest that in order to

~~CONFIDENTIAL~~

avoid drag penalties associated with the development of the second velocity peak into a second shock system on the upper surface at intermediate off-design conditions, the magnitude of the second peak should be less than that of the leading-edge peak.

Langley Research Center,
National Aeronautics and Space Administration,
Hampton, Va., December 1, 1971.

REFERENCES

1. Whitcomb, Richard T.; and Clark, Larry R.: An Airfoil Shape for Efficient Flight at Supercritical Mach Numbers. NASA TM X-1109, 1965.
2. Whitcomb, Richard T.; and Blackwell, James A., Jr.: Status of Research on a Super-critical Wing. Conference on Aircraft Aerodynamics, NASA SP-124, 1966, pp. 367-381.
3. Blackwell, James A., Jr.: Aerodynamic Characteristics of an 11-Percent-Thick Symmetrical Supercritical Airfoil at Mach Numbers Between 0.30 and 0.85. NASA TM X-1831, 1969.
4. Harris, Charles D.: Wind-Tunnel Investigation of Effects of Trailing-Edge Geometry on a NASA Supercritical Airfoil Section. NASA TM X-2336, 1971.
5. Baals, Donald D.; and Mourhess, Mary J.: Numerical Evaluation of the Wake-Survey Equations for Subsonic Flow Including the Effect of Energy Addition. NACA WR L-5, 1945. (Formerly NACA ARR L5H27.)
6. Schaefer, William T., Jr.: Characteristics of Major Active Wind Tunnels at the Langley Research Center. NASA TM X-1130, 1965.
7. Blackwell, James A., Jr.: Preliminary Study of Effects of Reynolds Number and Boundary-Layer Transition Location on Shock-Induced Separation. NASA TN D-5003, 1969.
8. Davis, Don D., Jr.; and Moore, Dewey: Analytical Study of Blockage- and Lift-Interference Corrections for Slotted Tunnels Obtained by the Substitution of an Equivalent Homogeneous Boundary for the Discrete Slots. NACA RM L53E07b, 1953.

~~CONFIDENTIAL~~

TABLE I.- SECTION COORDINATES OF SUPERCRITICAL AIRFOIL 5
[$c = 63.0$ cm (24.8 in.)]

x/c	y/c		m	
	Upper	Lower	Upper	Lower
0.0065	0.0158	-0.0157	1.000	-1.024
.0125	.0203	-.0206	.612	-.669
.0250	.0267	-.0271	.376	-.419
.0375	.0302	-.0316	.280	-.311
.050	.0334	-.0351	.225	-.248
.075	.0381	-.0403	.161	-.174
.100	.0416	-.0440	.124	-.130
.125	.0444	-.0469	.098	-.100
.150	.0466	-.0491	.080	-.078
.175	.0484	-.0508	.065	-.060
.200	.0499	-.0521	.054	-.047
.250	.0521	-.0539	.036	-.025
.300	.0536	-.0548	.023	-.010
.350	.0545	-.0549	.012	.008
.400	.0548	-.0541	.001	.025
.450	.0549	-.0524	-.006	.043
.500	.0544	-.0497	-.014	.067
.550	.0534	-.0455	-.023	.104
.575	.0529	-.0426	-.028	.131
.600	.0519	-.0389	-.032	.166
.625	.0512	-.0342	-.038	.211
.650	.0502	-.0285	-.044	.244
.675	.0490	-.0224	-.051	.249
.700	.0477	-.0165	-.058	.225
.725	.0461	-.0112	-.067	.201
.750	.0443	-.0065	-.077	.177
.775	.0422	-.0024	-.089	.152
.800	.0398	.0011	-.104	.126
.825	.0370	.0039	-.120	.096
.850	.0338	.0059	-.140	.063
.875	.0300	.0070	-.164	.023
.900	.0256	.0069	-.191	-.026
.925	.0204	.0056	-.223	-.087
.950	.0144	.0024	-.260	-.164
.975	.0074	-.0028	-.302	-.260
1.000	-.0008	-.0108	-.352	-.381
L.E. radius: 0.0223c				

TABLE II. - SECTION COORDINATES OF SUPERCRITICAL AIRFOIL 6

 $[c = 63.0 \text{ cm} (24.8 \text{ in.})]$

x/c	y/c		m	
	Upper	Lower	Upper	Lower
.0065	0.0158	-0.0157	1.000	-1.024
.0125	.0203	-.0206	.612	-.669
.0250	.0267	-.0271	.376	-.419
.0375	.0302	-.0316	.280	-.311
.0500	.0334	-.0351	.225	-.248
.0750	.0381	-.0403	.161	-.174
.100	.0416	-.0440	.124	-.130
.125	.0444	-.0469	.098	-.100
.150	.0466	-.0491	.080	-.078
.175	.0484	-.0508	.065	-.061
.200	.0499	-.0521	.054	-.047
.250	.0521	-.0539	.036	-.026
.300	.0536	-.0548	.023	-.010
.350	.0545	-.0549	.012	.008
.400	.0549	-.0541	.003	.025
.450	.0548	-.0524	-.006	.043
.500	.0544	-.0497	-.016	.067
.550	.0533	-.0455	-.026	.104
.575	.0526	-.0426	-.031	.131
.600	.0516	-.0389	-.036	.166
.625	.0508	-.0342	-.042	.211
.650	.0497	-.0285	-.048	.244
.675	.0484	-.0224	-.055	.249
.700	.0469	-.0165	-.063	.225
.725	.0452	-.0112	-.072	.201
.750	.0433	-.0065	-.082	.177
.775	.0411	-.0024	-.093	.152
.800	.0386	.0011	-.107	.126
.825	.0358	.0039	-.122	.096
.850	.0325	.0059	-.141	.063
.875	.0287	.0070	-.162	.023
.900	.0244	.0069	-.187	-.026
.925	.0194	.0056	-.215	-.087
.950	.0136	.0024	-.249	-.164
.975	.0069	-.0028	-.287	-.260
1.000	-.0008	-.0108	-.331	-.381
L.E. radius: 0.0223c				

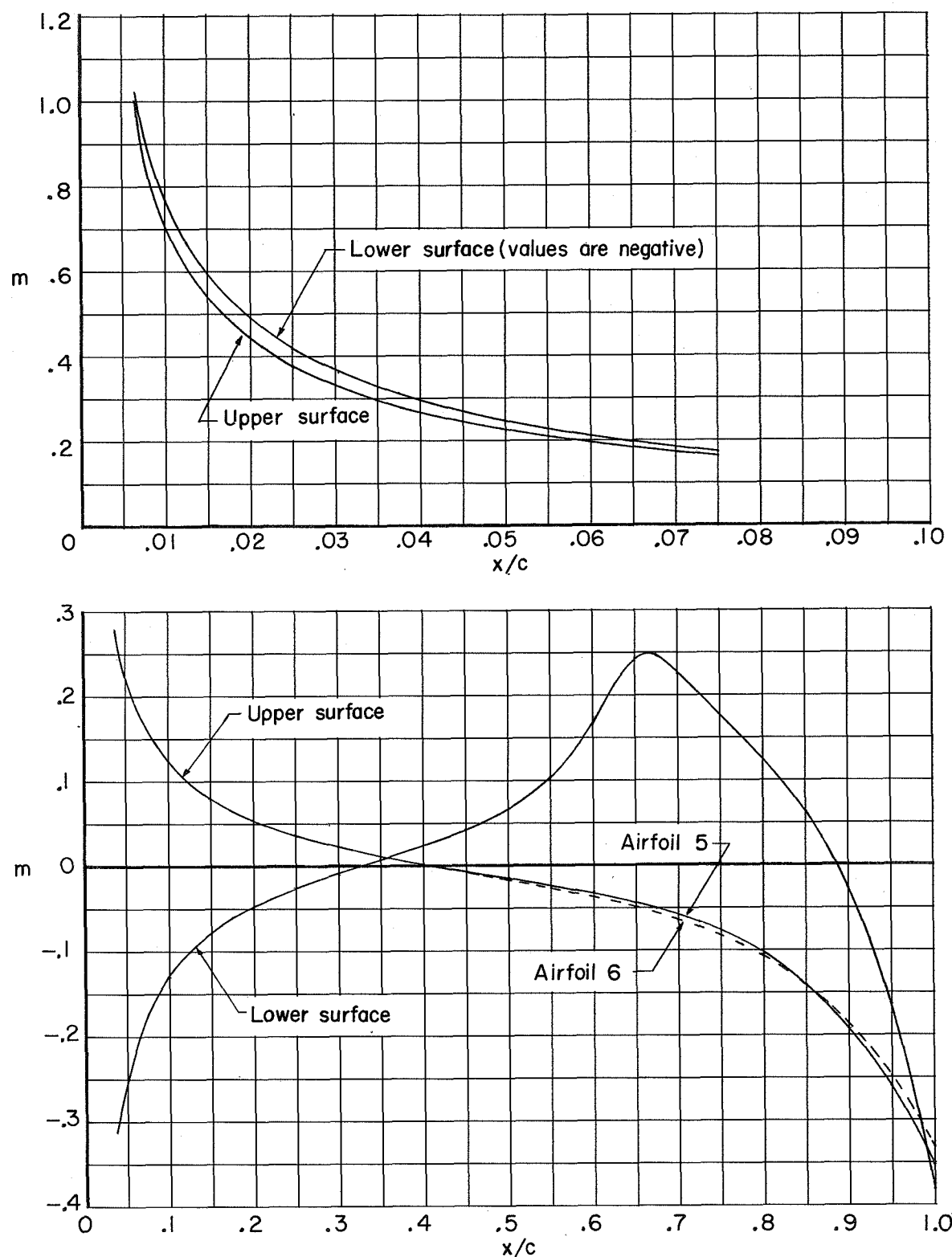
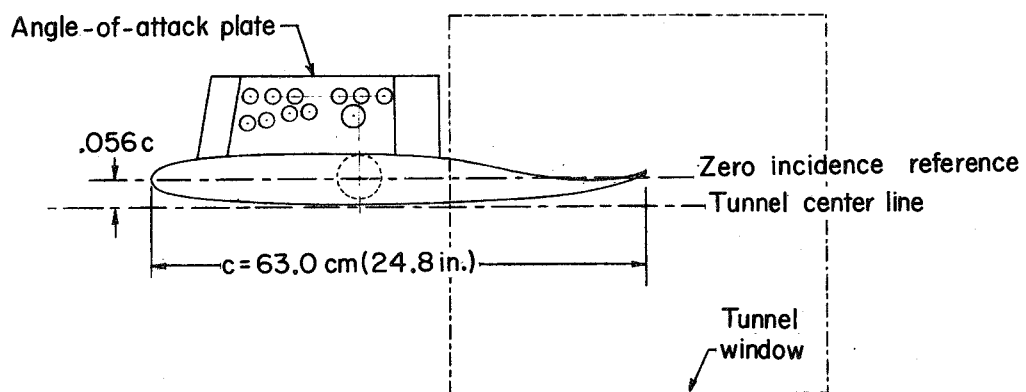
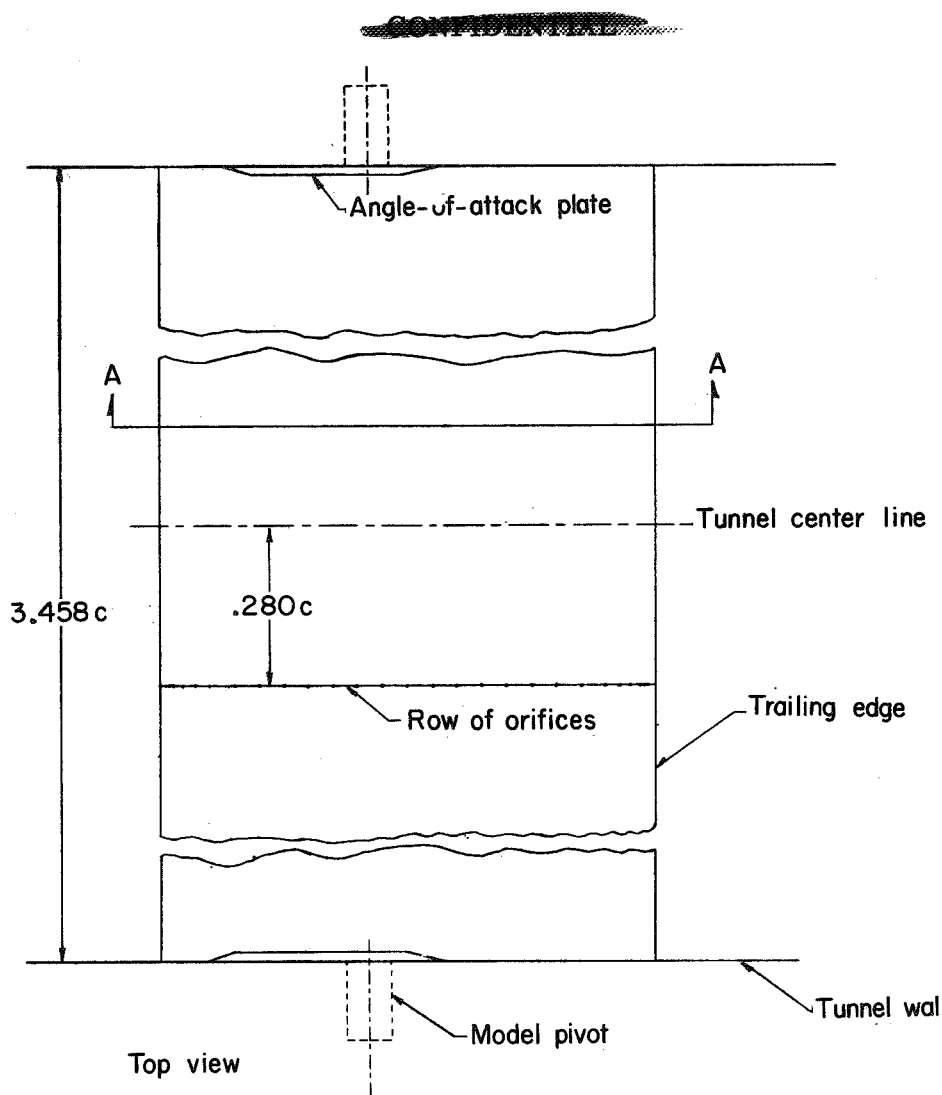


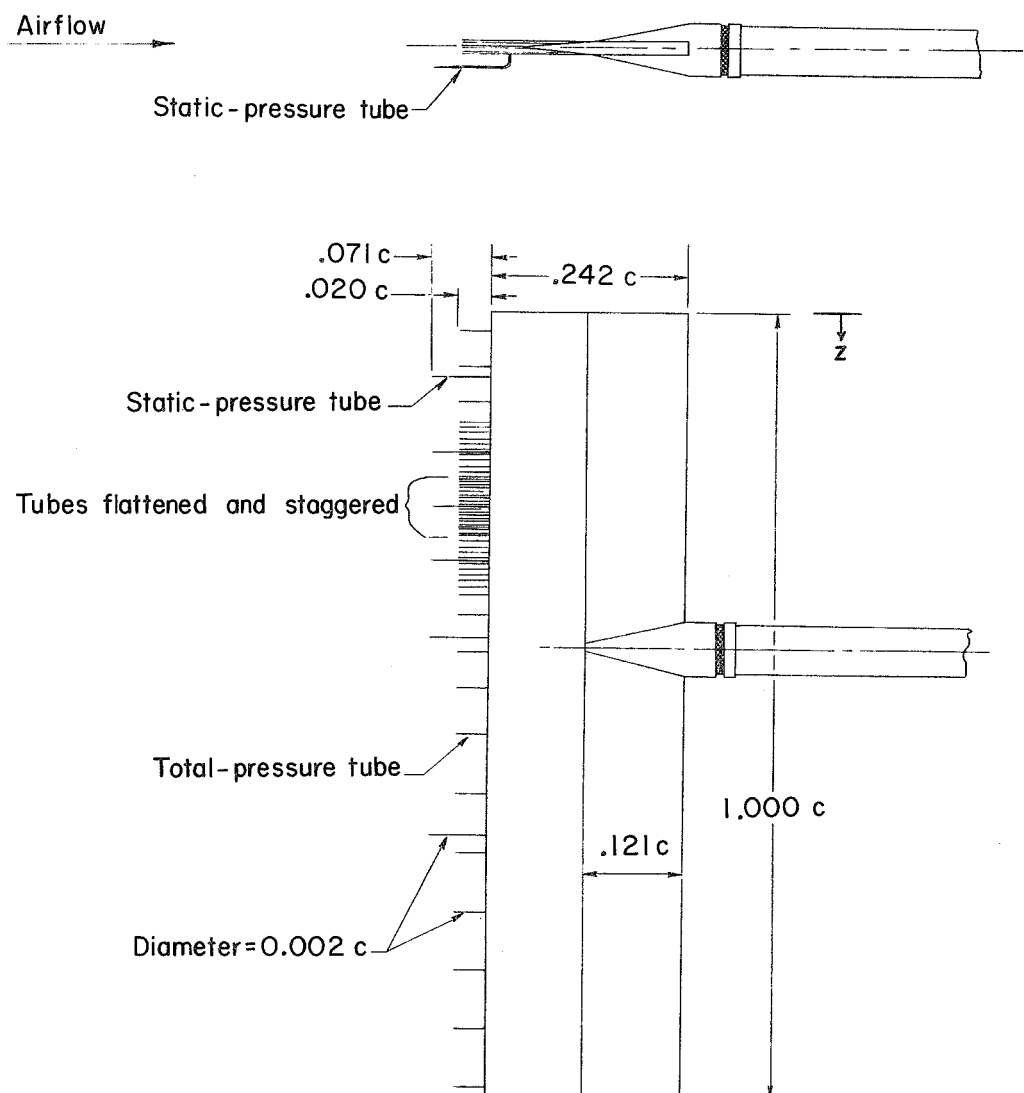
Figure 1.- Chordwise distribution of slopes.



End view, section A-A

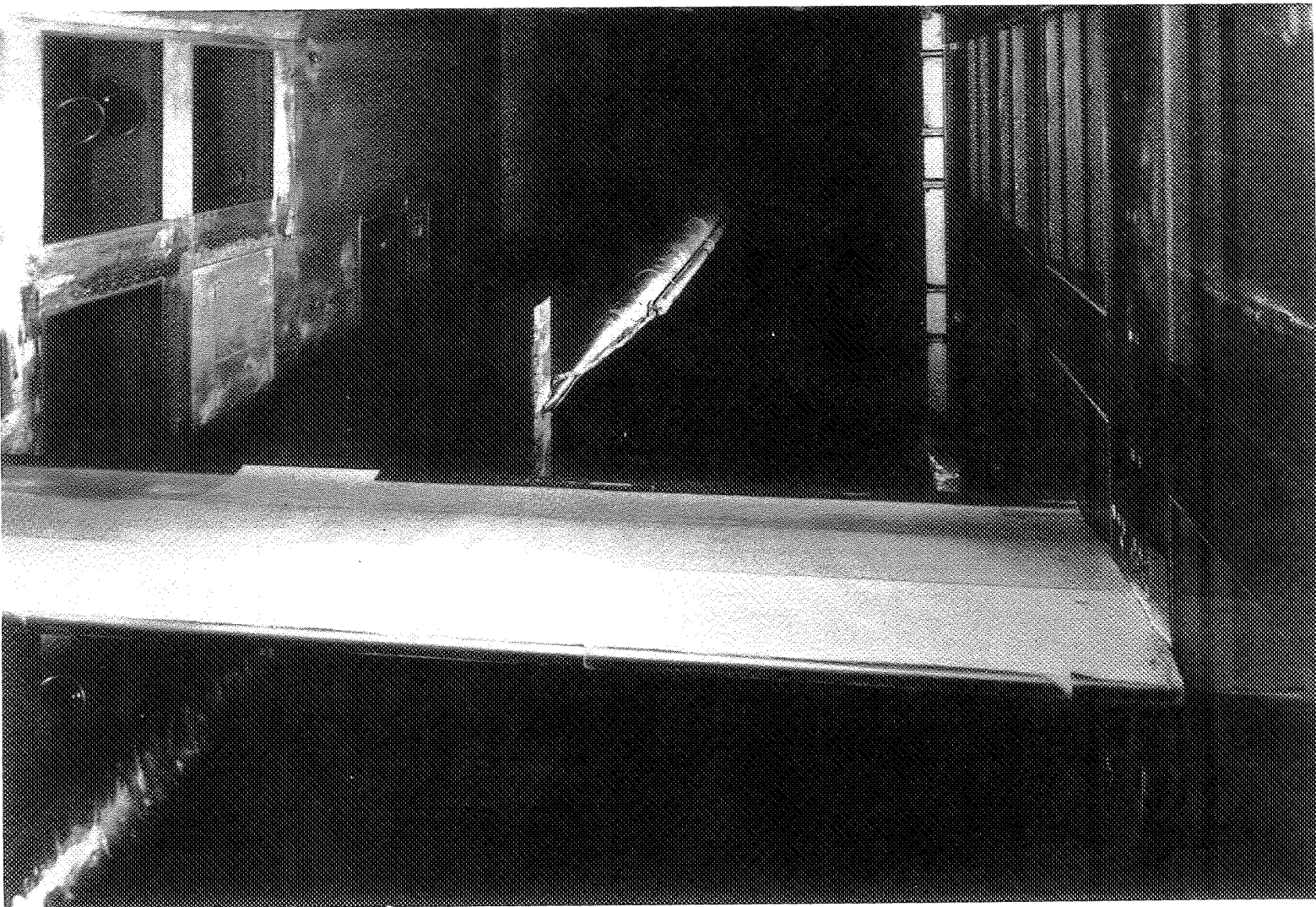
(a) Airfoil mounted in tunnel.

Figure 2.- Apparatus.



(b) Profile drag rake.

Figure 2.- Concluded.



L-67-5566

Figure 3.- Supercritical airfoil and profile drag rake in Langley 8-foot transonic pressure tunnel.

~~CONFIDENTIAL~~

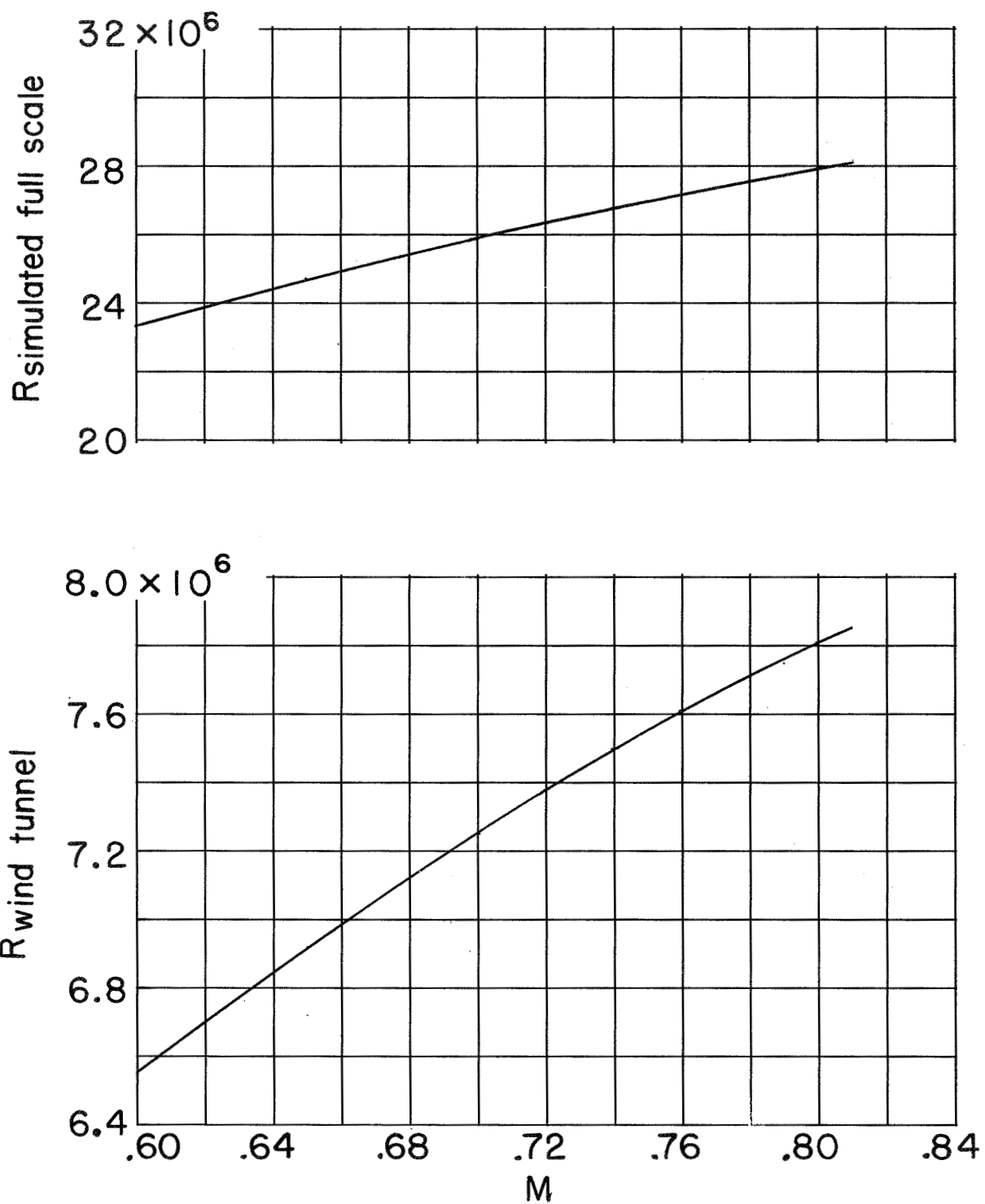
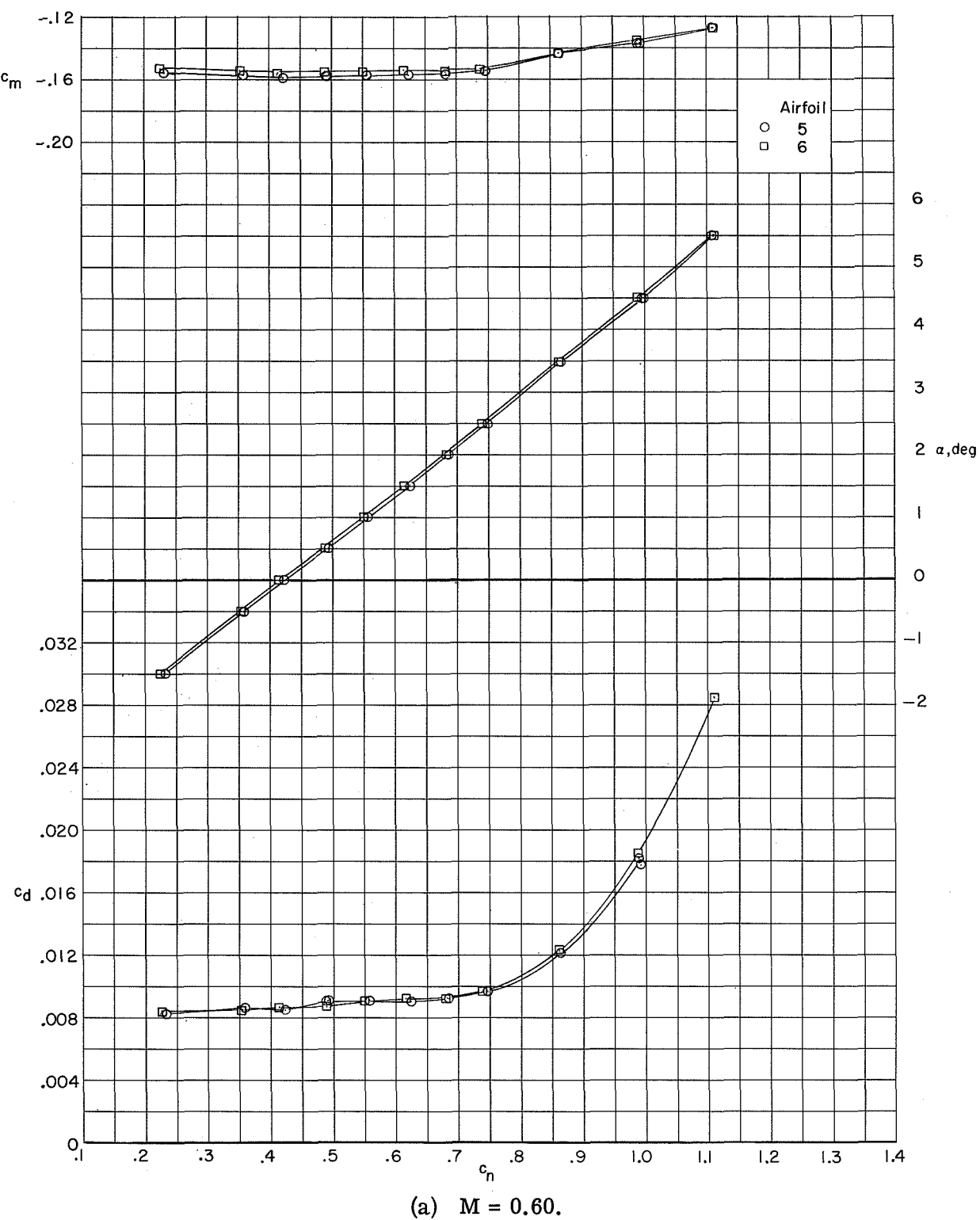
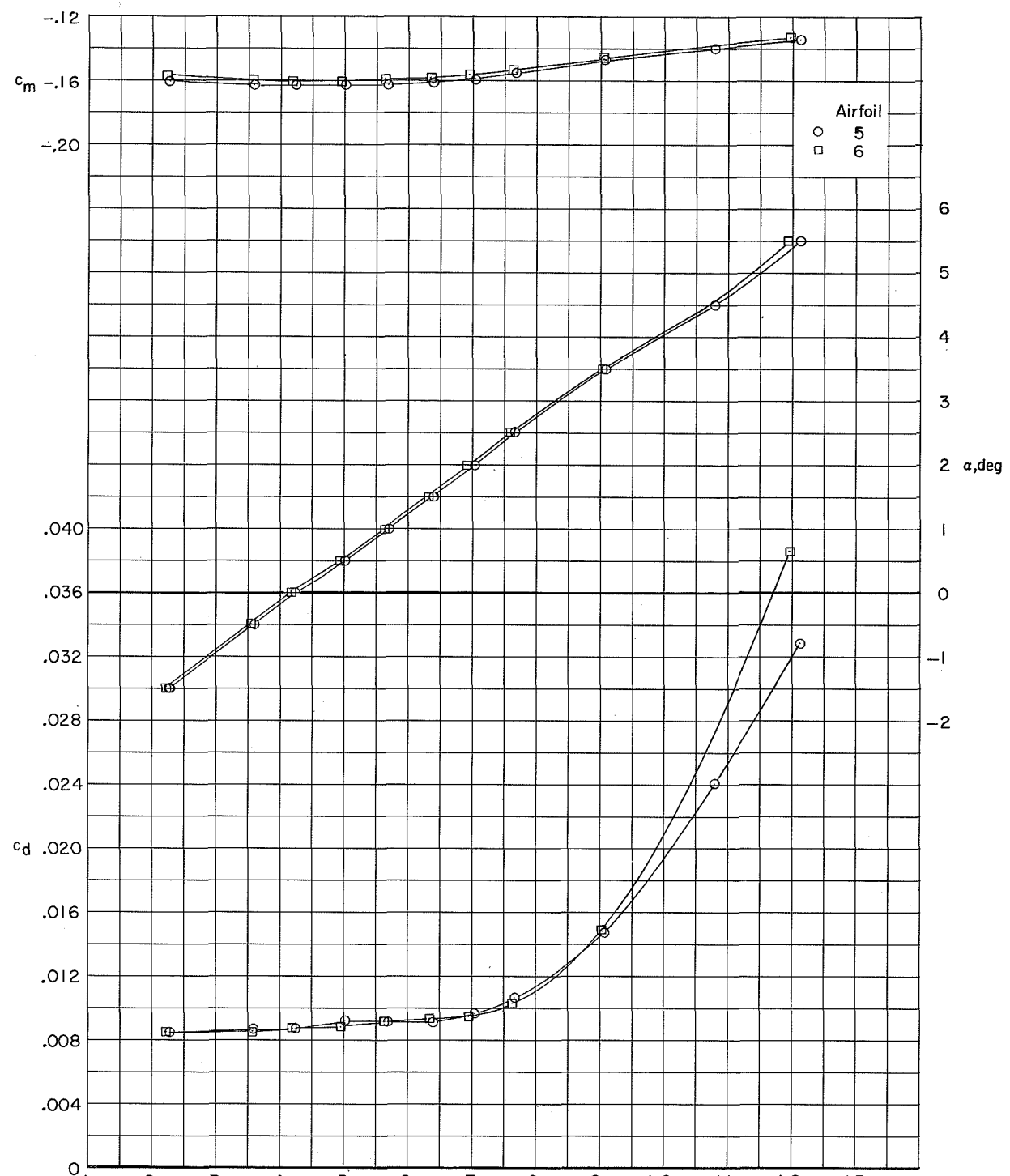


Figure 4.- Variation of test Reynolds number with Mach number.



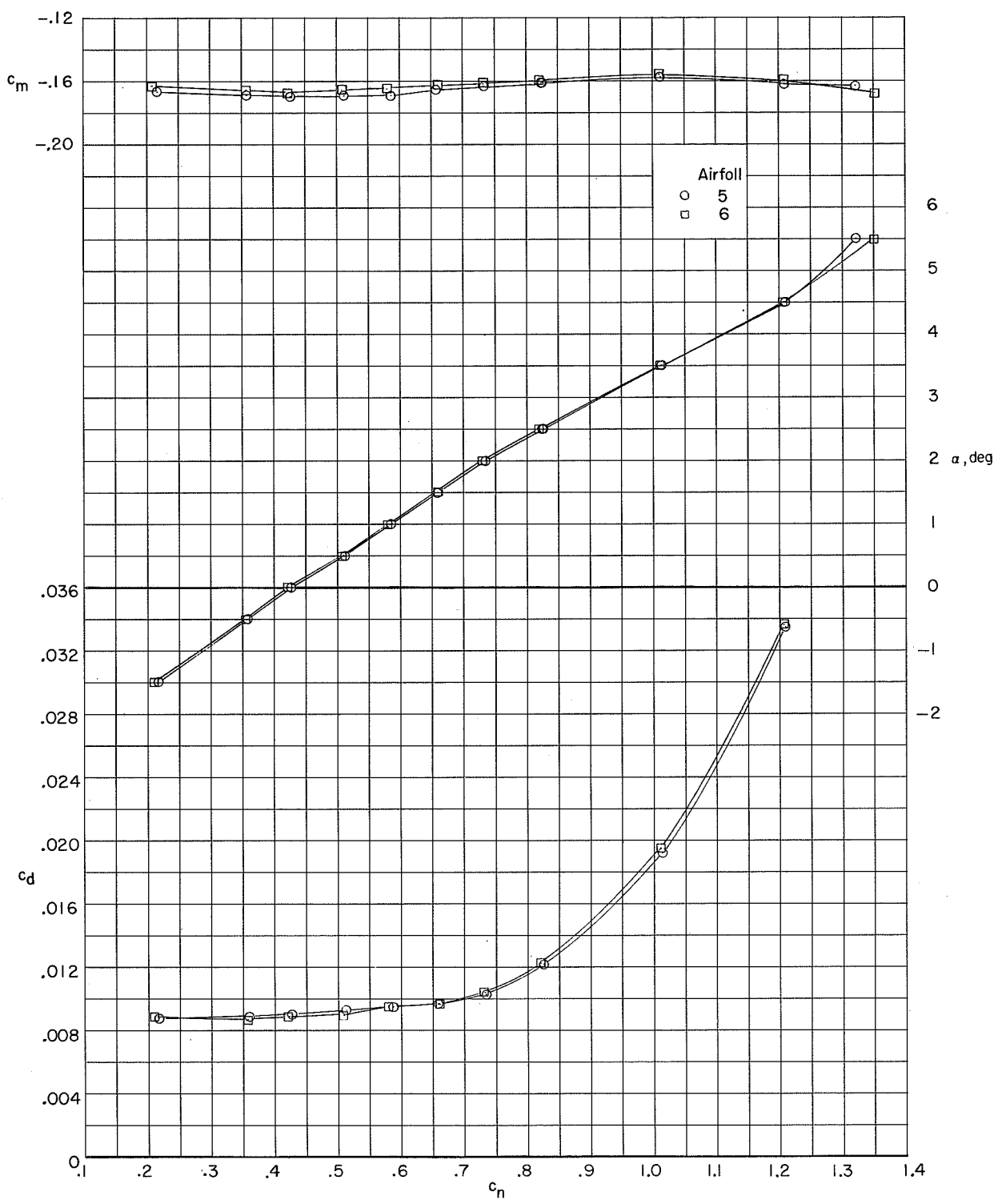
(a) $M = 0.60$.

Figure 5.- Effect of upper surface modification on variation of section pitching-moment coefficient, angle of attack, and section drag coefficient with section normal-force coefficient.



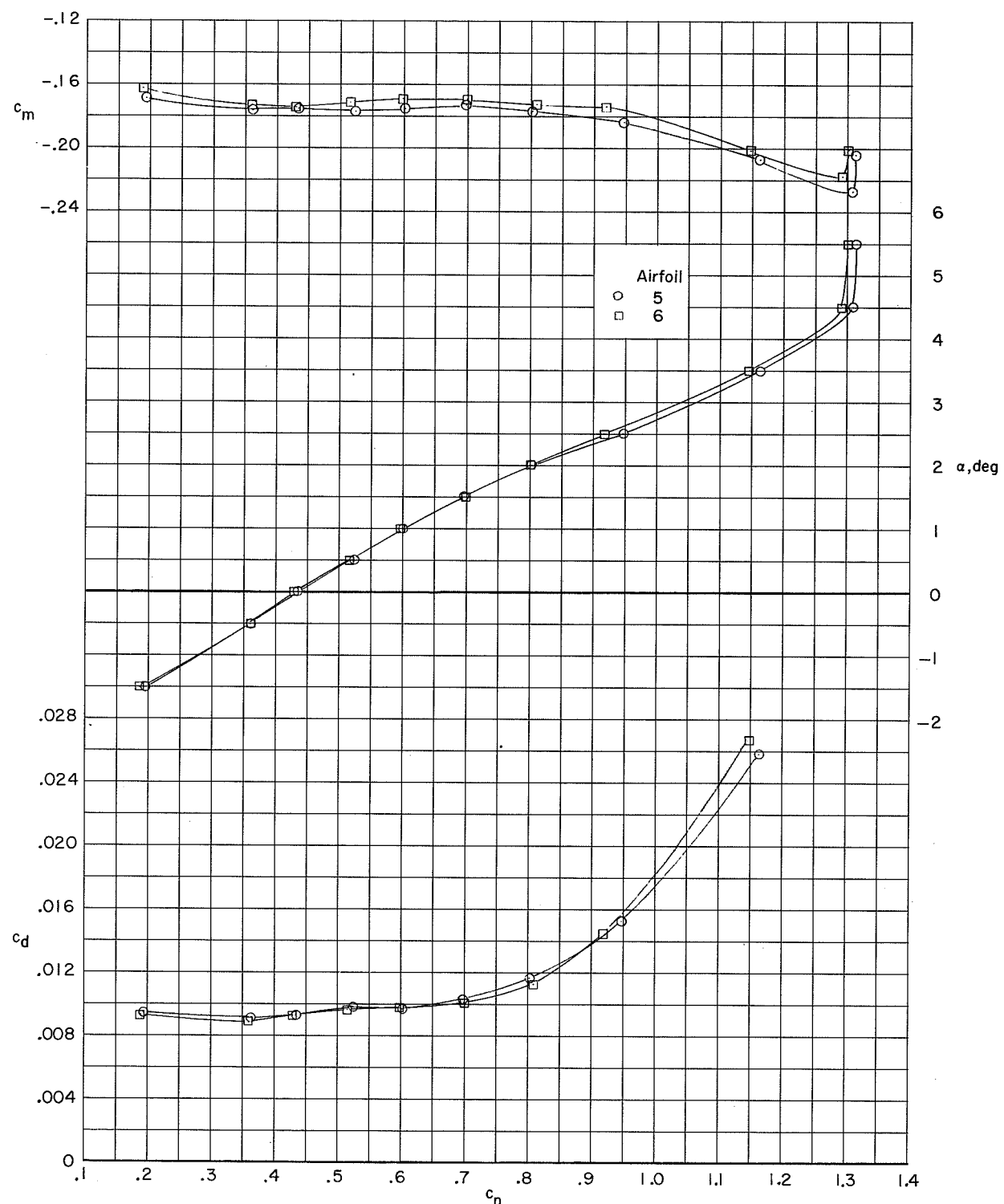
(b) $M = 0.65$.

Figure 5.- Continued.



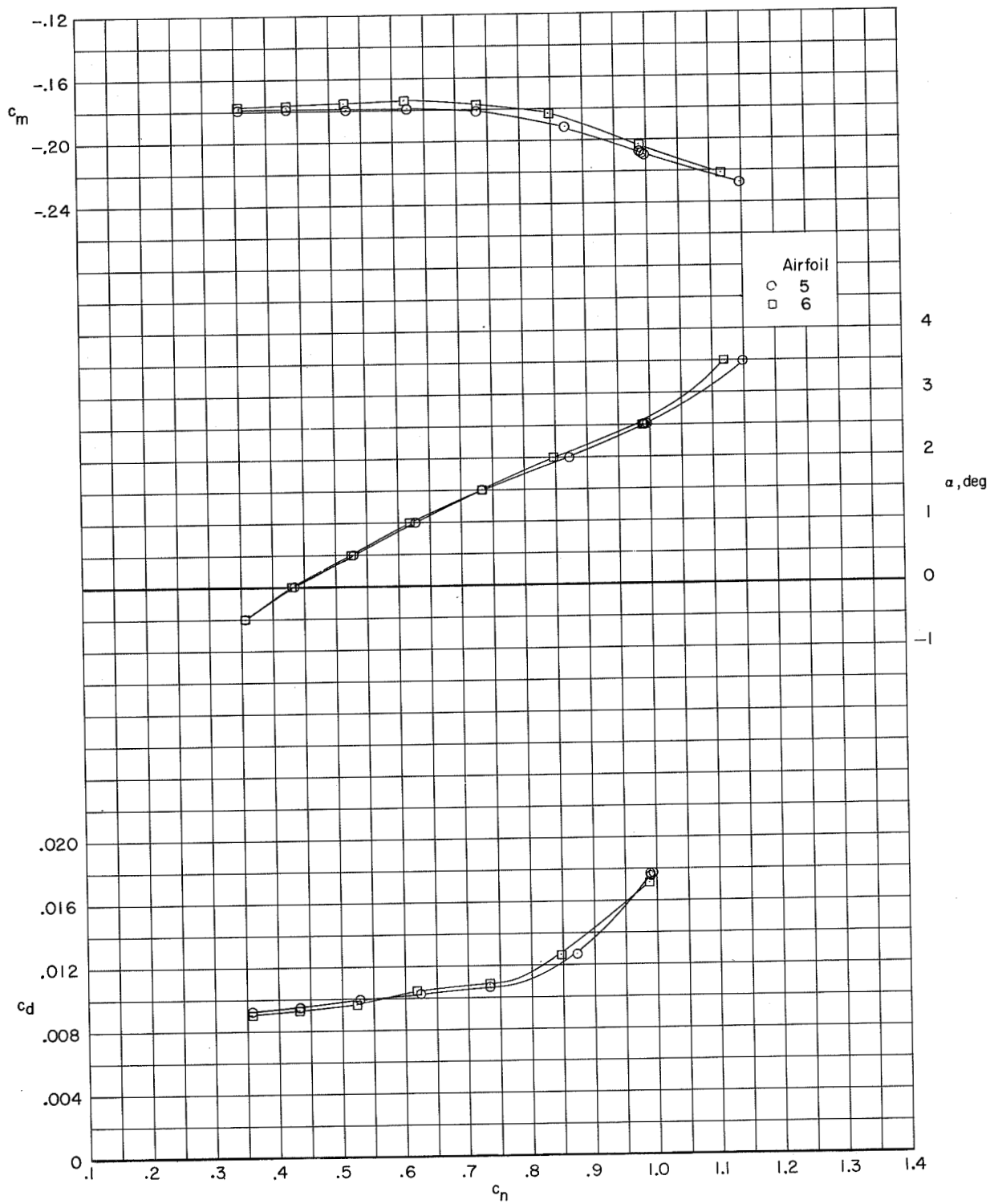
(c) $M = 0.70$.

Figure 5.- Continued.



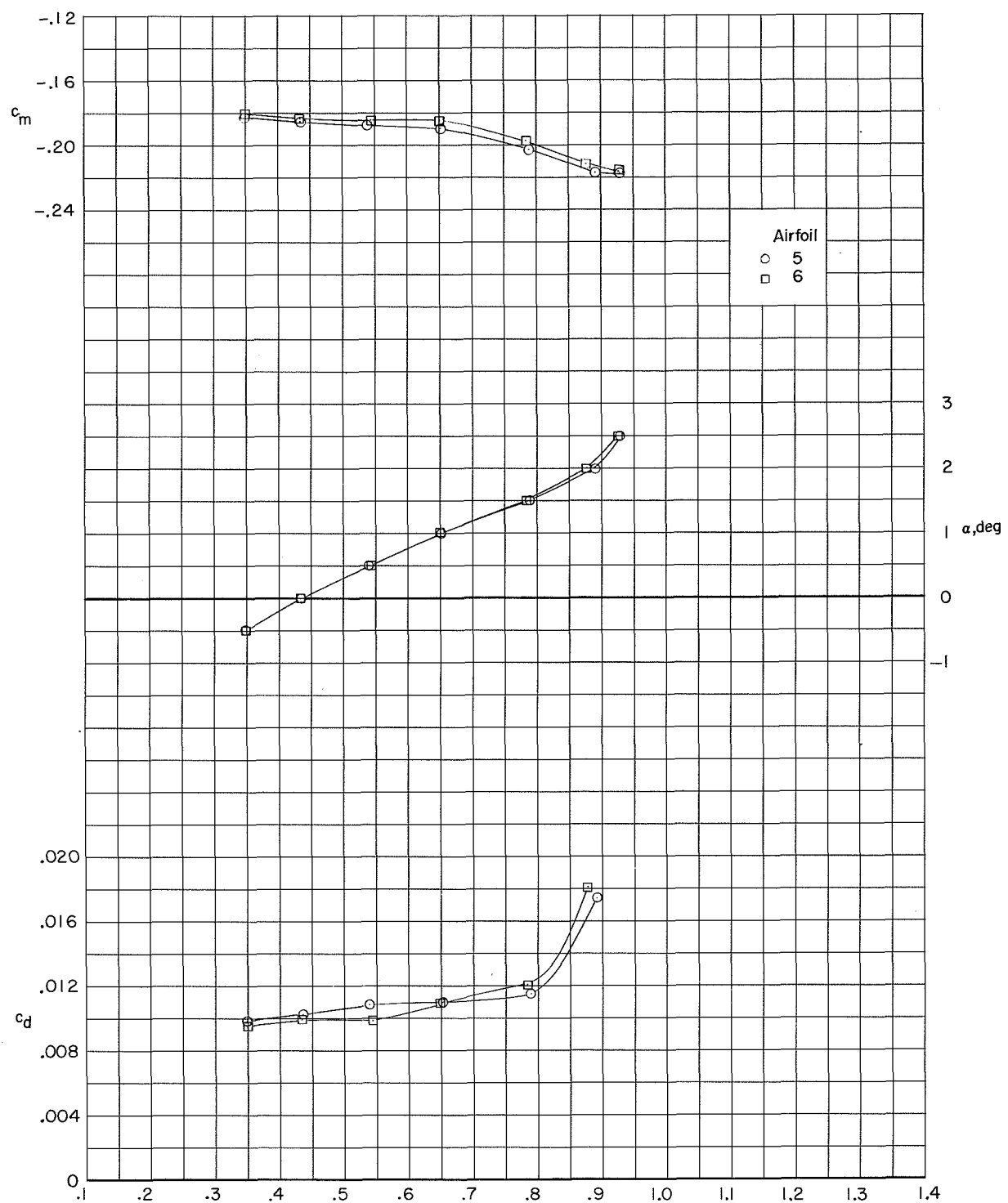
(d) $M = 0.74$.

Figure 5.- Continued.



(e) $M = 0.76$.

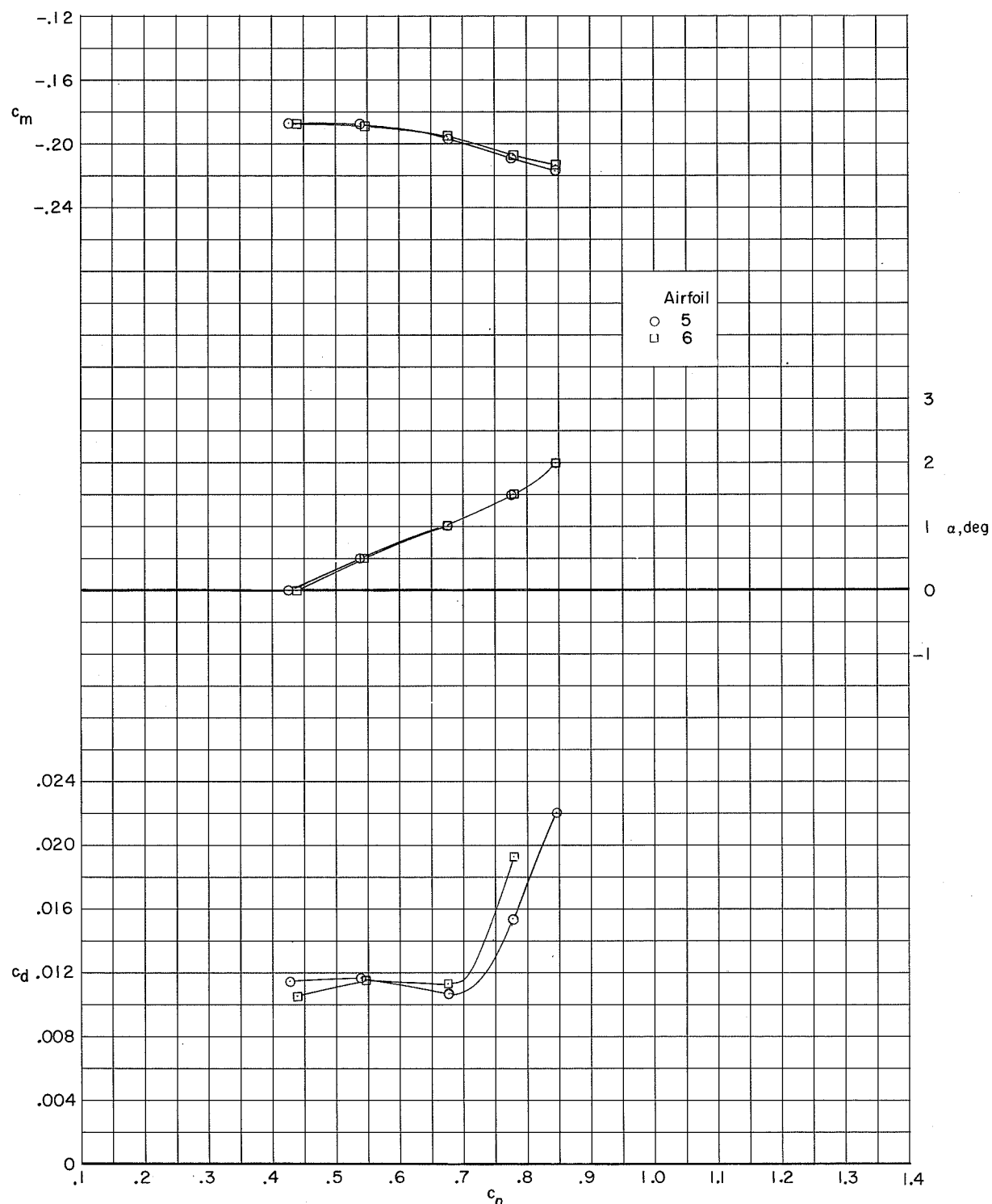
Figure 5.- Continued.



(f) $M = 0.78$.

Figure 5.- Continued.

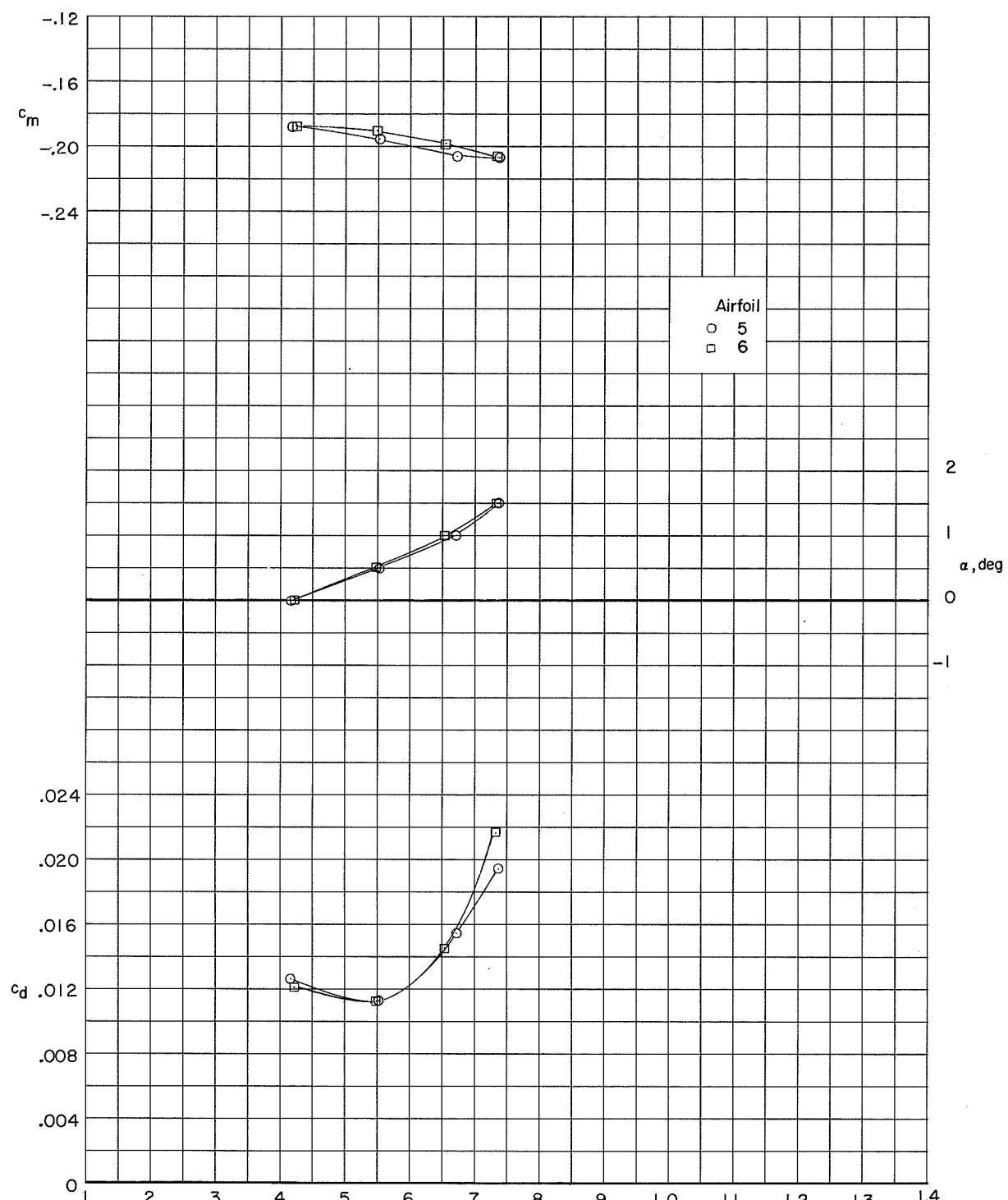
~~CONFIDENTIAL~~



(g) $M = 0.79$.

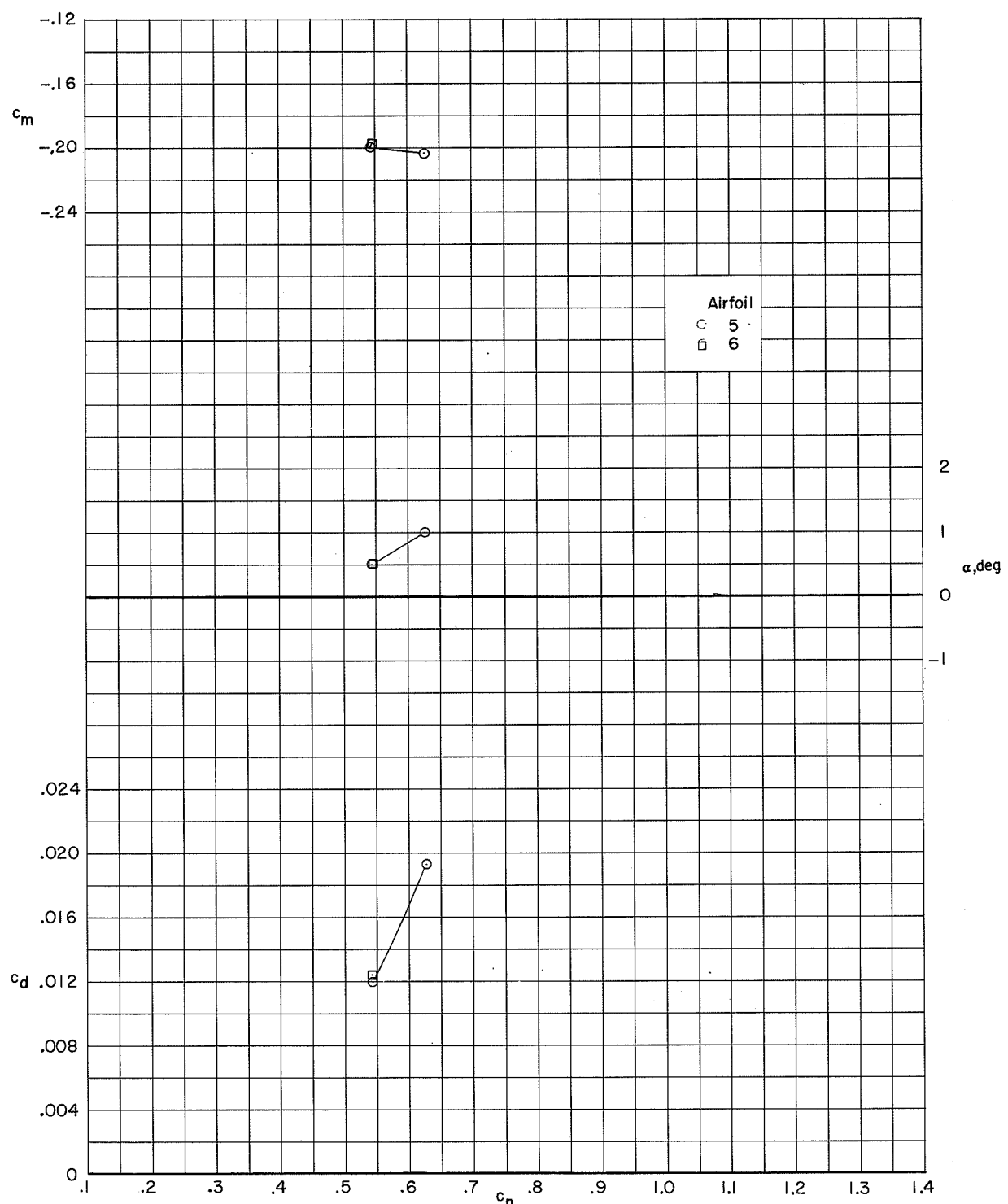
Figure 5.- Continued.

~~CONFIDENTIAL~~



(h) $M = 0.80$.

Figure 5.- Continued.



(i) $M = 0.81$.

Figure 5.- Concluded.

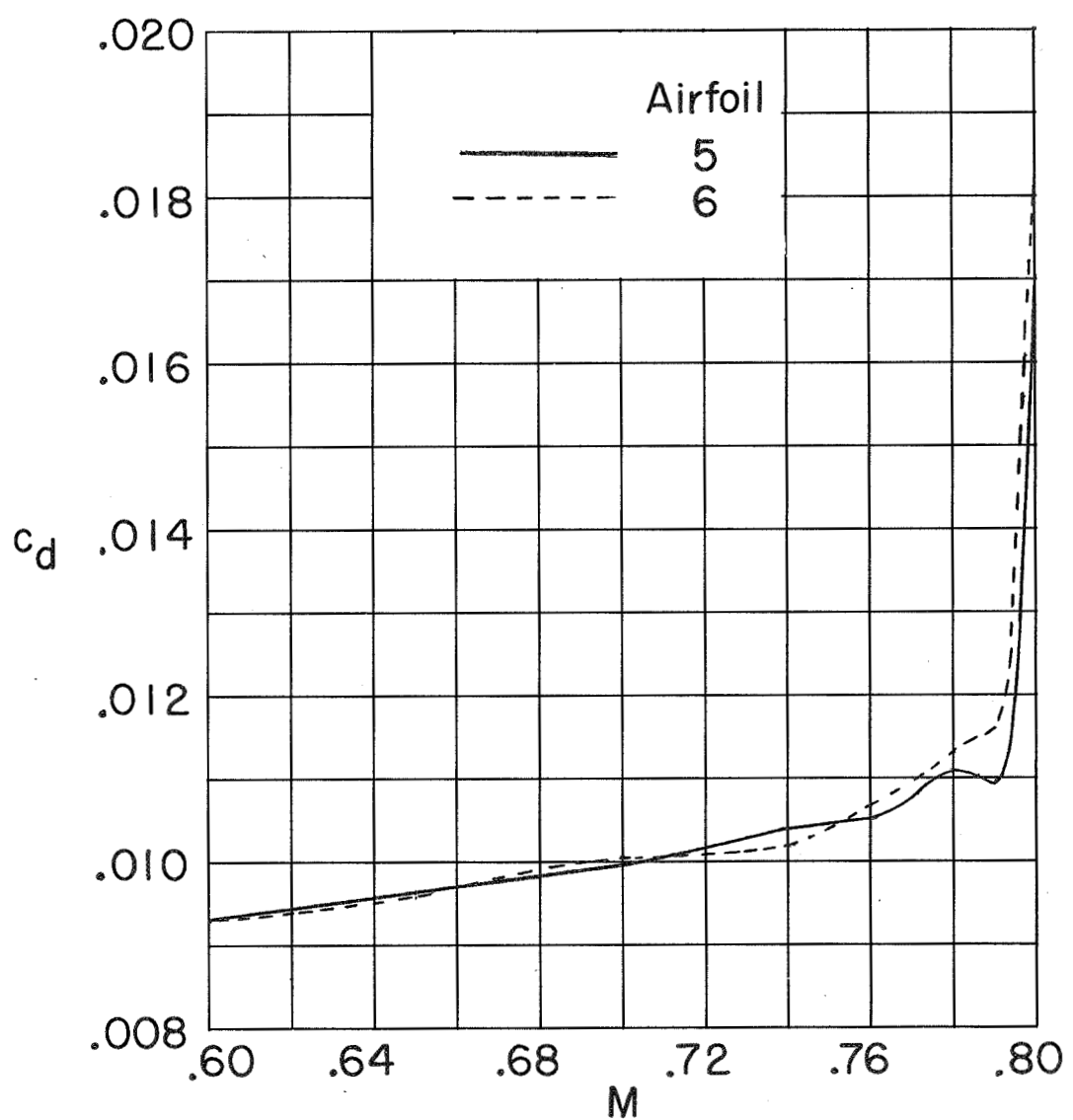
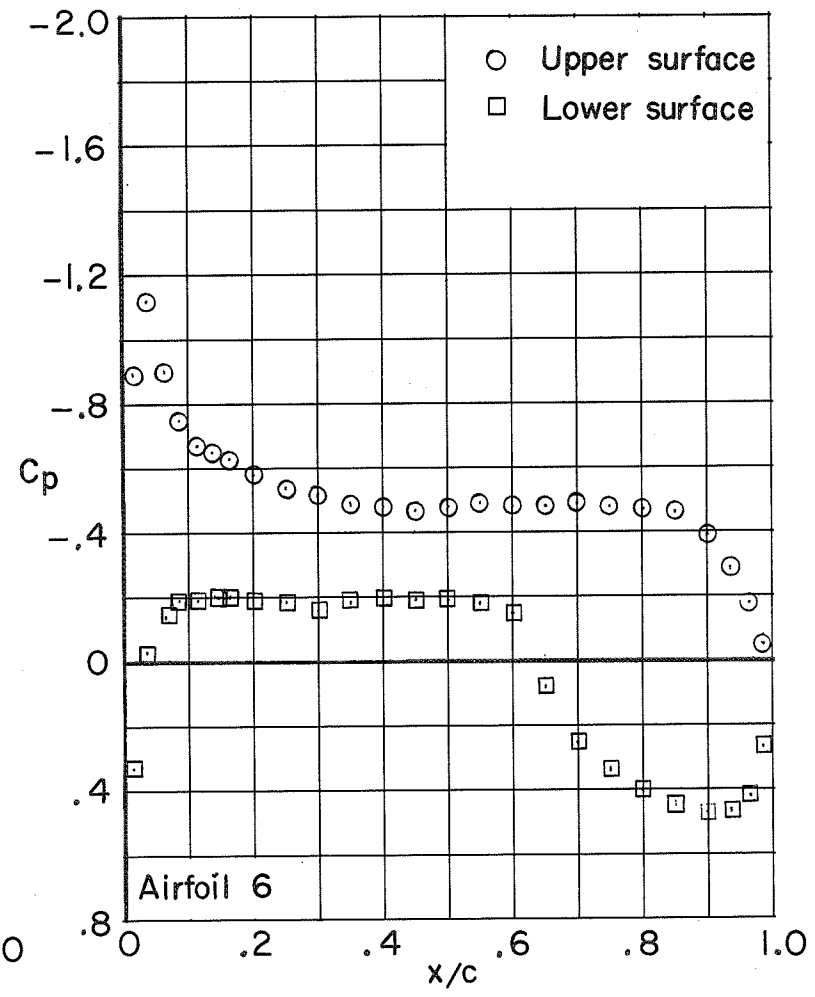
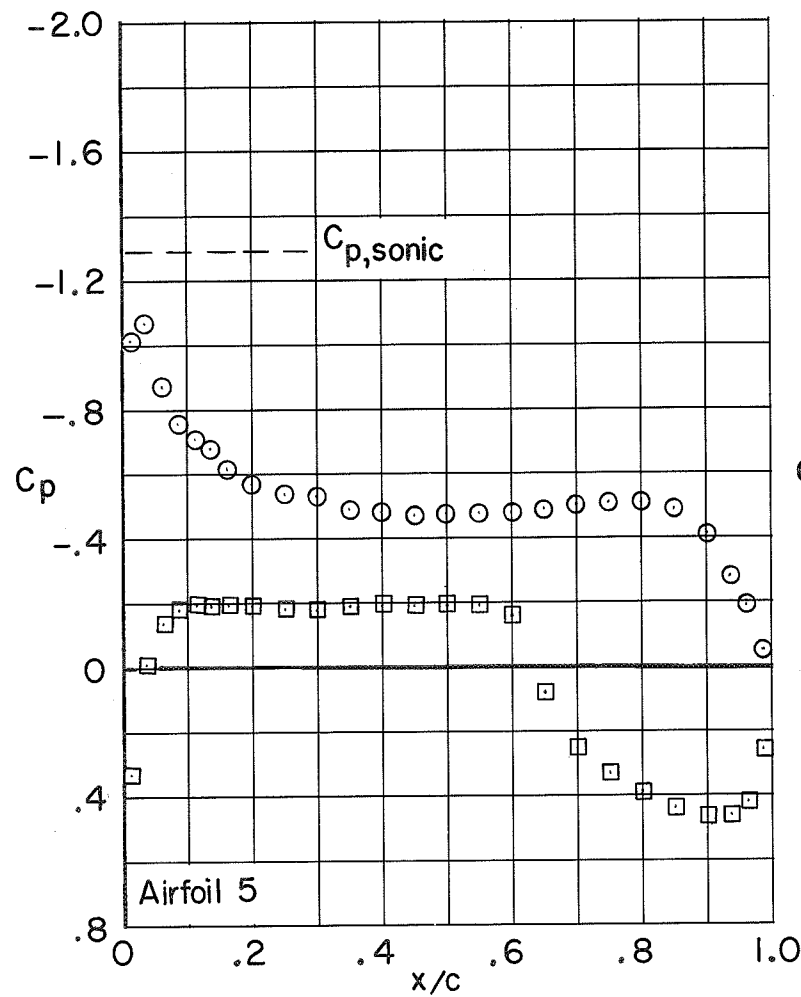
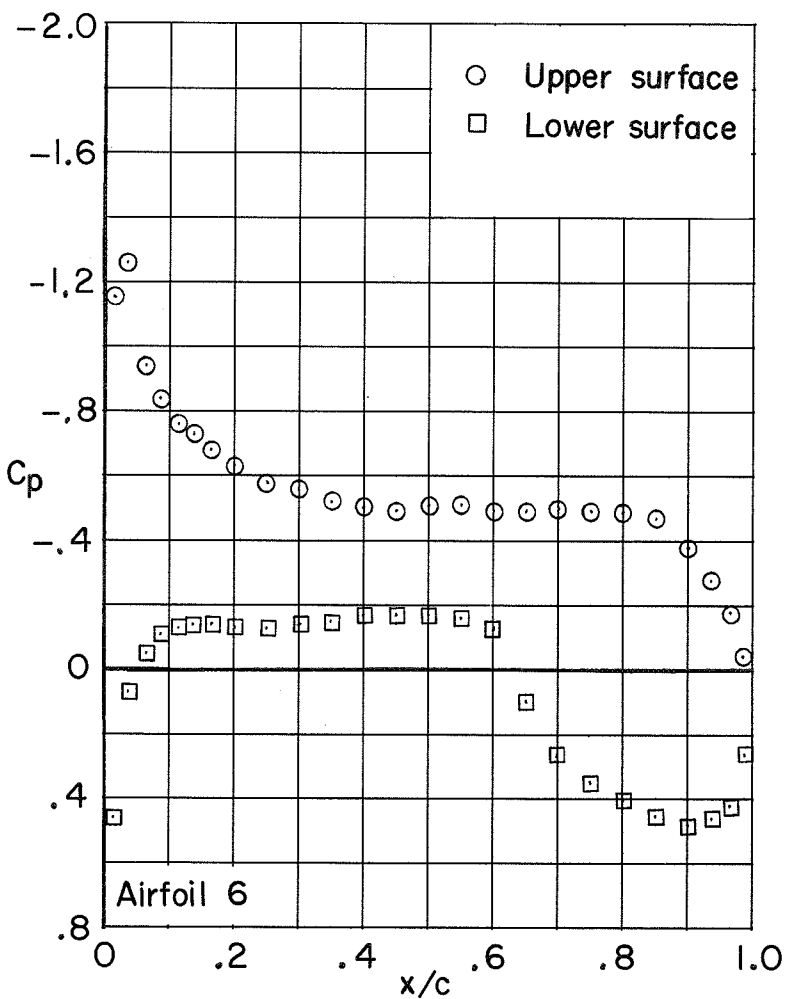
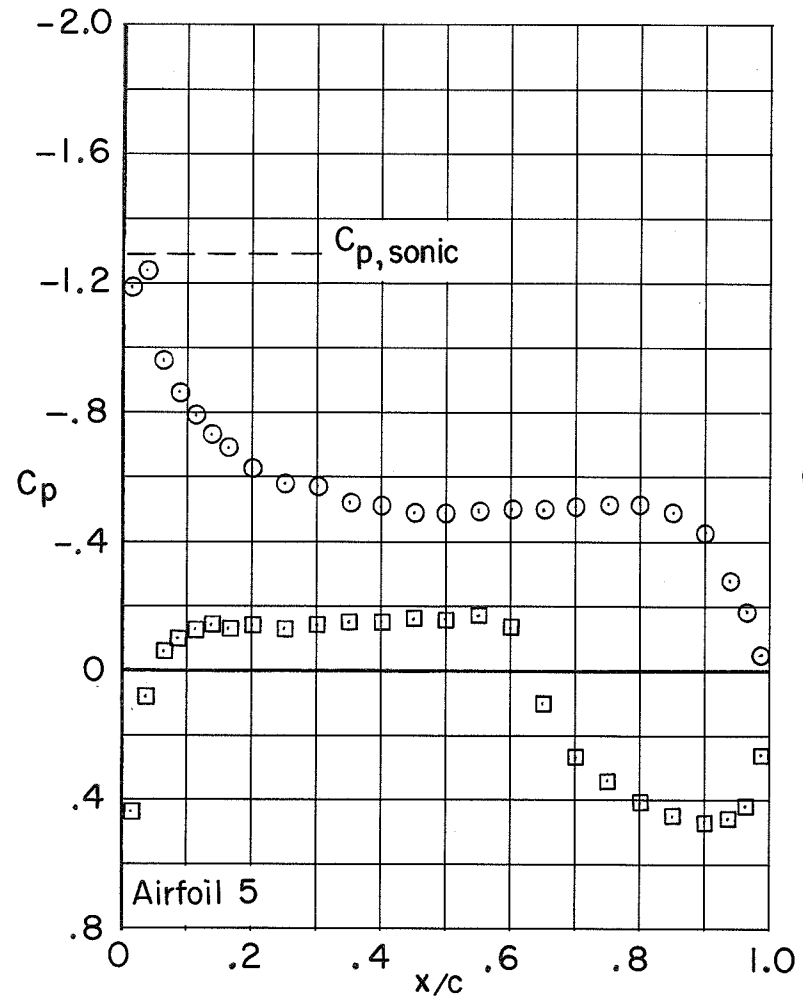


Figure 6.- Variation of section drag coefficient with Mach number at the design normal-force coefficient of 0.7.



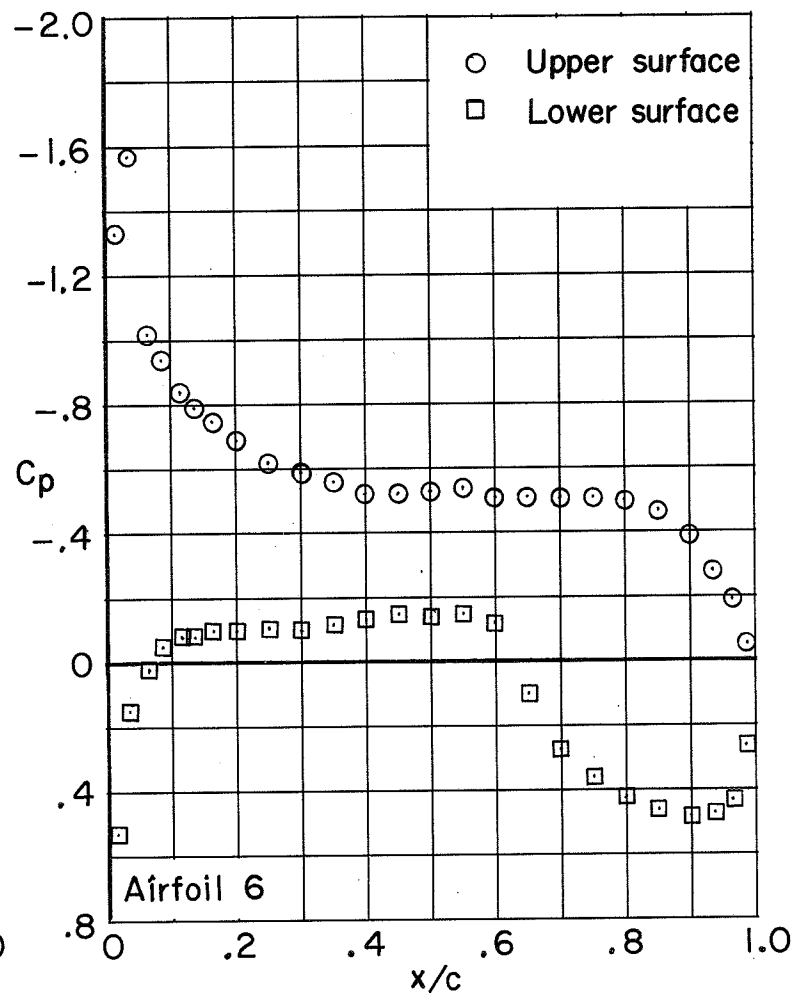
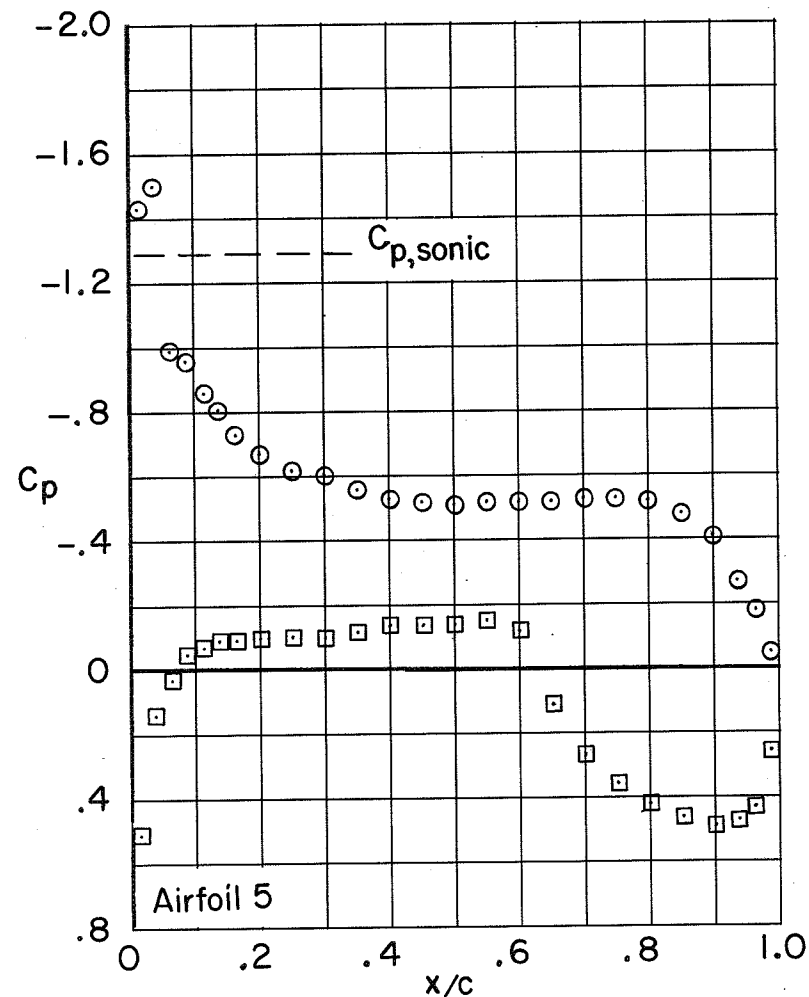
(a) $M = 0.60$; $\alpha = 1.0^\circ$.

Figure 7.- Comparison of chordwise pressure profiles of basic (airfoil 5) and modified (airfoil 6) airfoils.



(b) $M = 0.60$; $\alpha = 1.5^\circ$.

Figure 7.- Continued.



(c) $M = 0.60$; $\alpha = 2.0^\circ$.

Figure 7.- Continued.

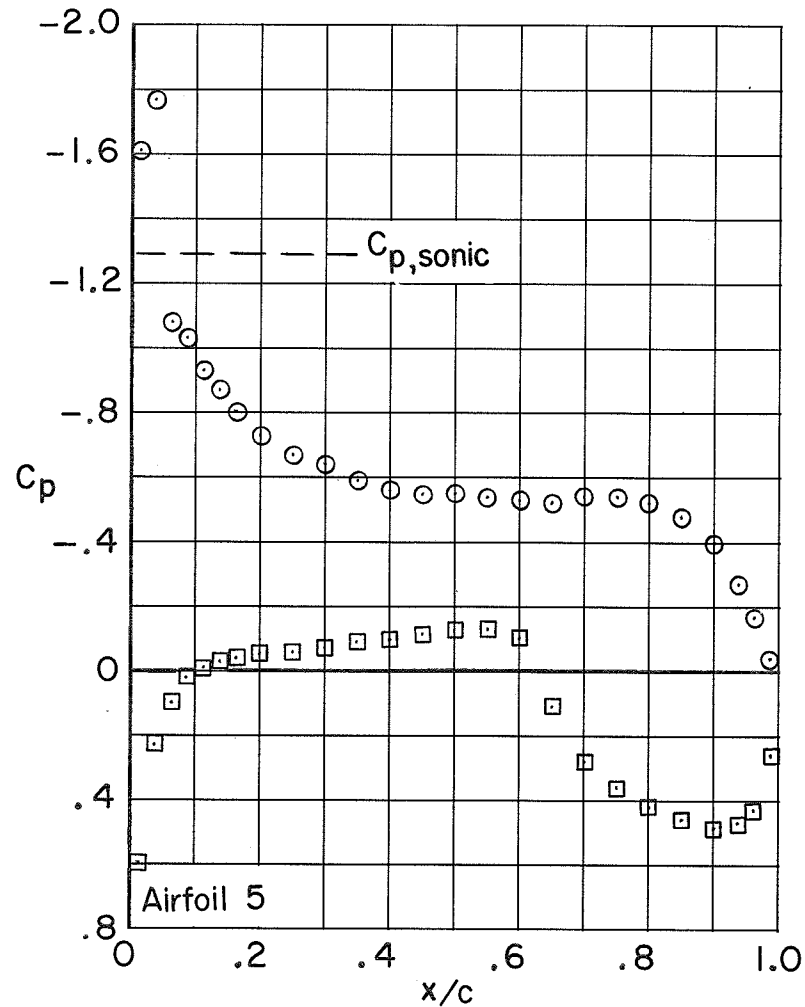
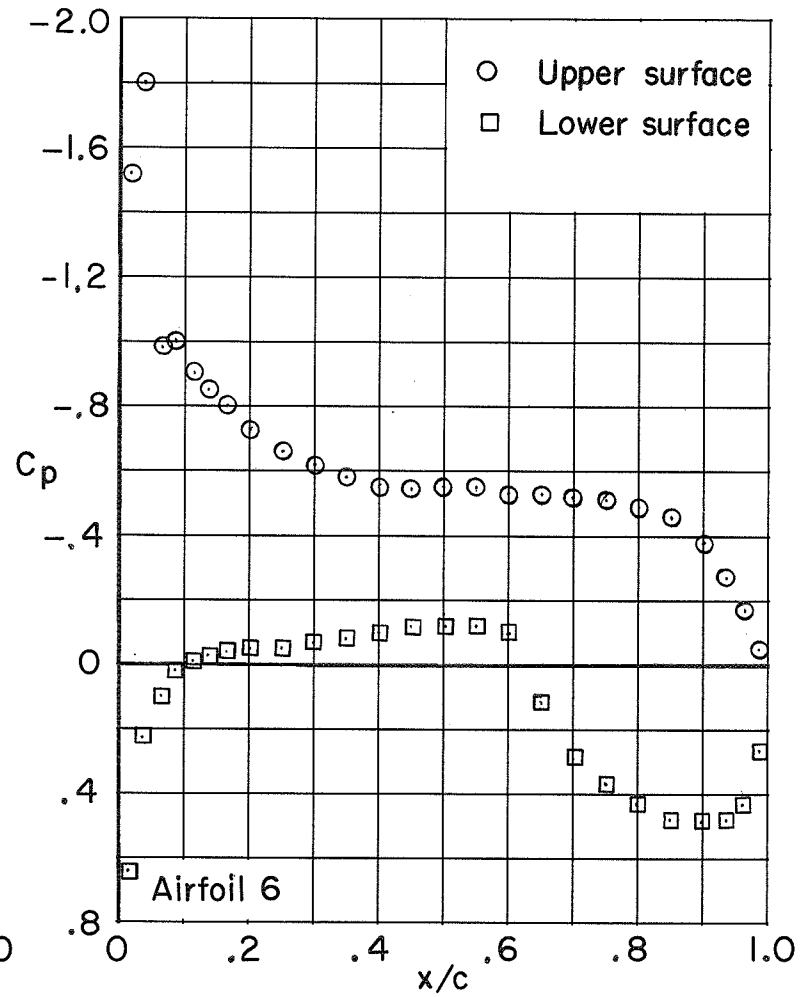
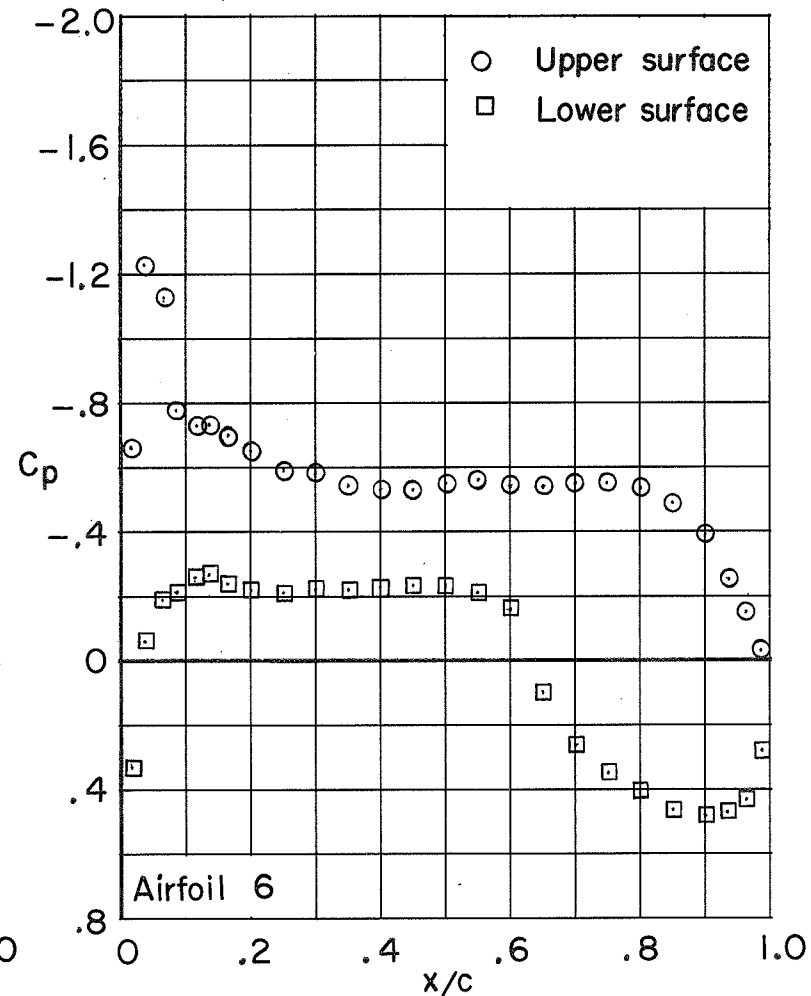
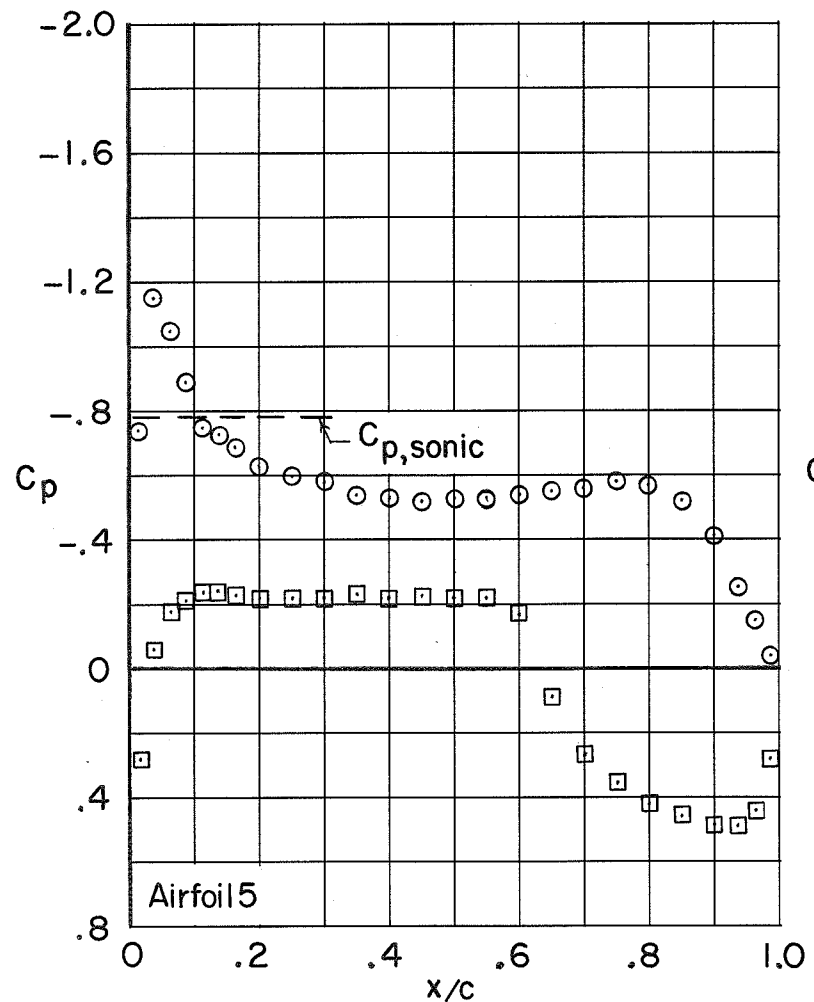
(d) $M = 0.60$; $\alpha = 2.5^\circ$.

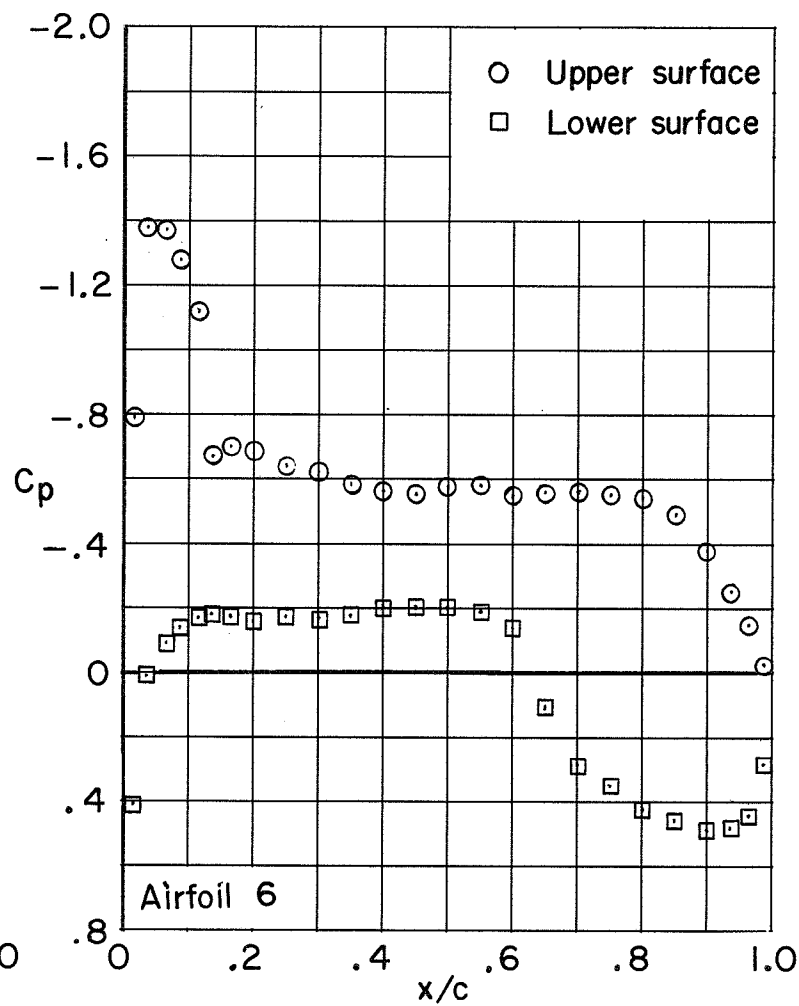
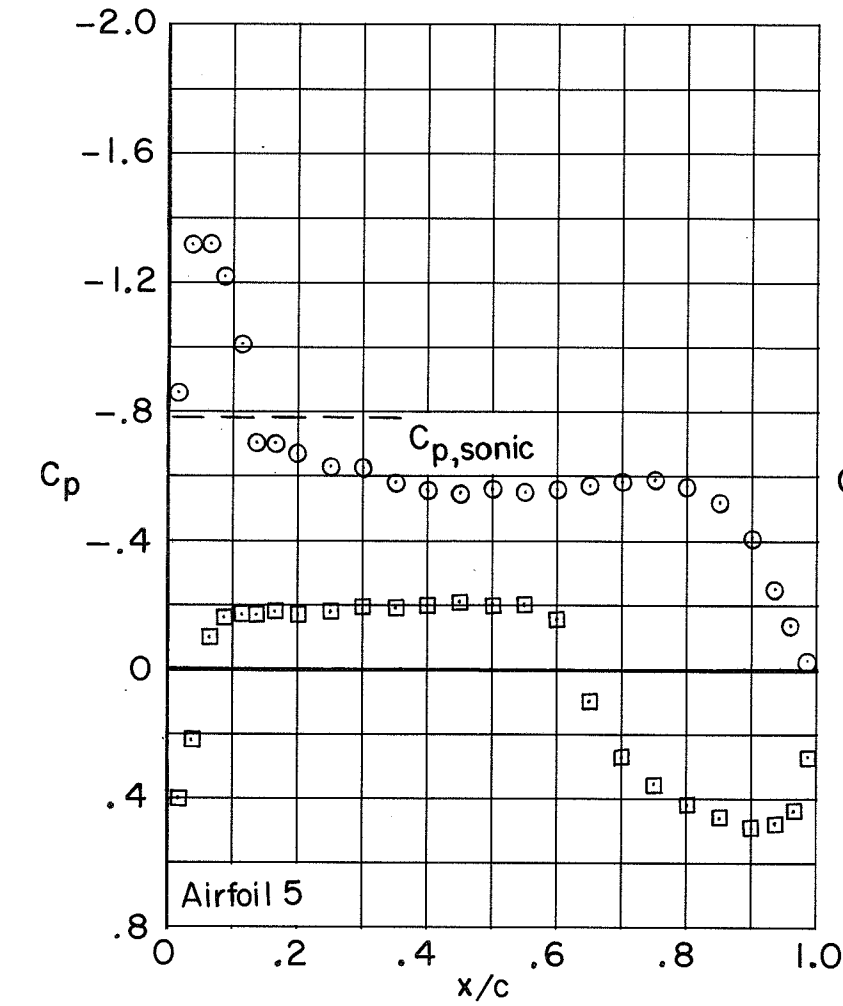
Figure 7.- Continued.





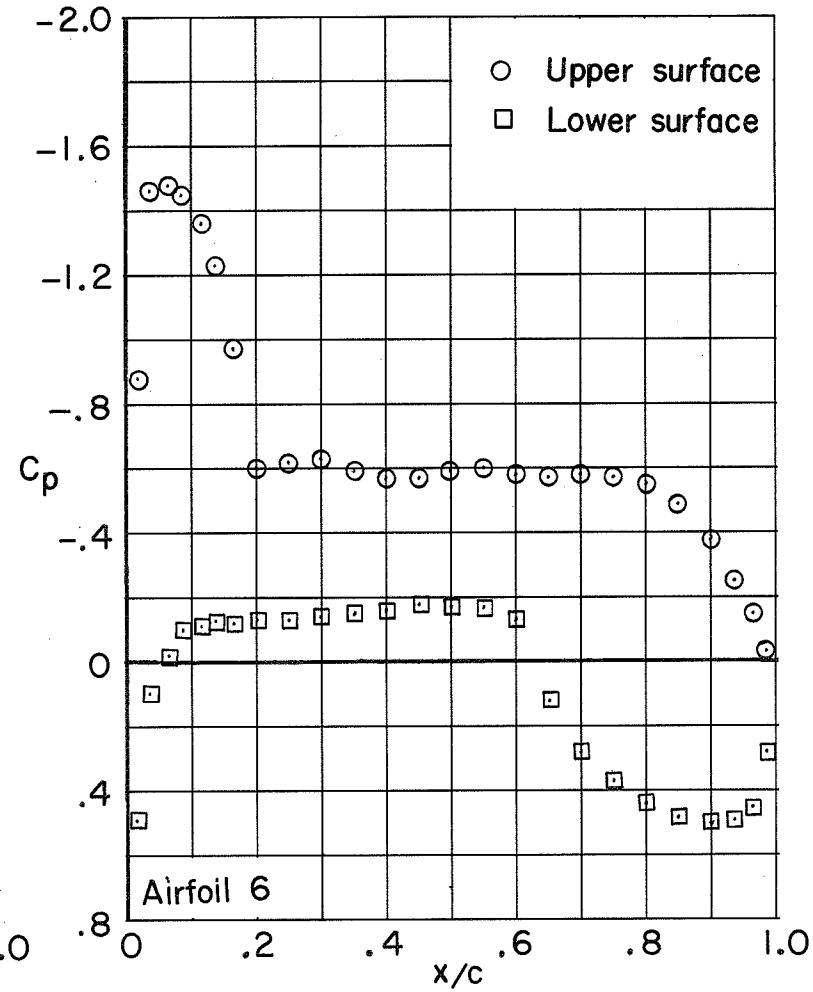
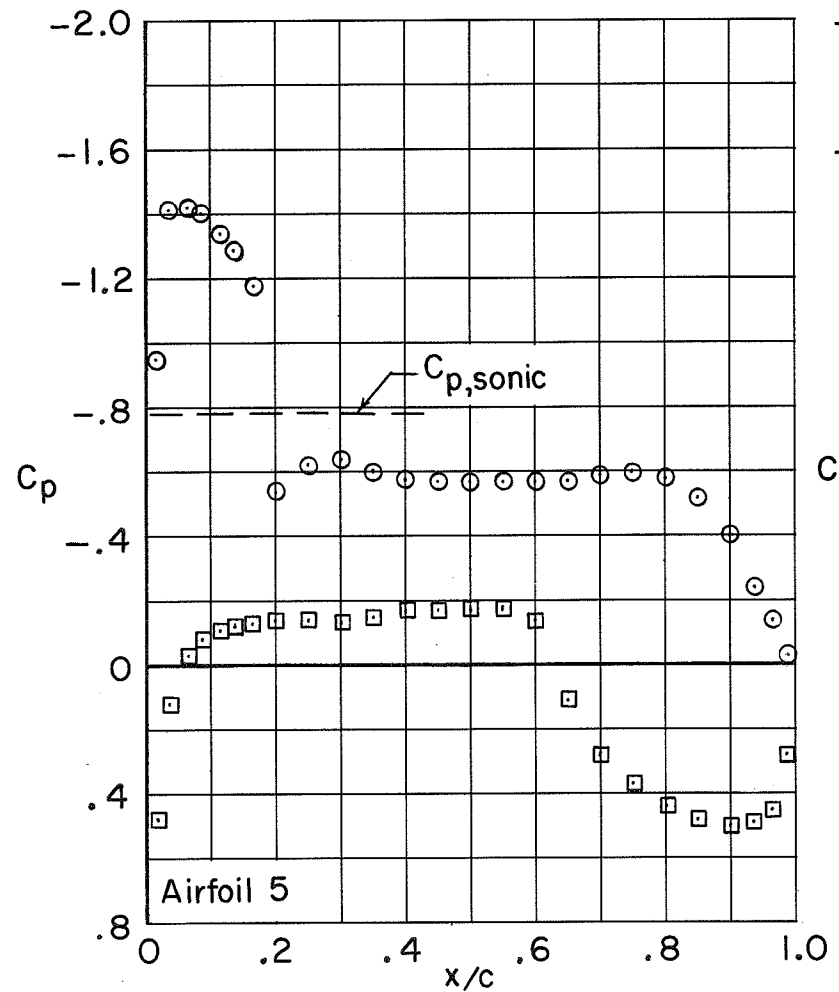
(e) $M = 0.70$; $\alpha = 1.0^\circ$.

Figure 7.- Continued.



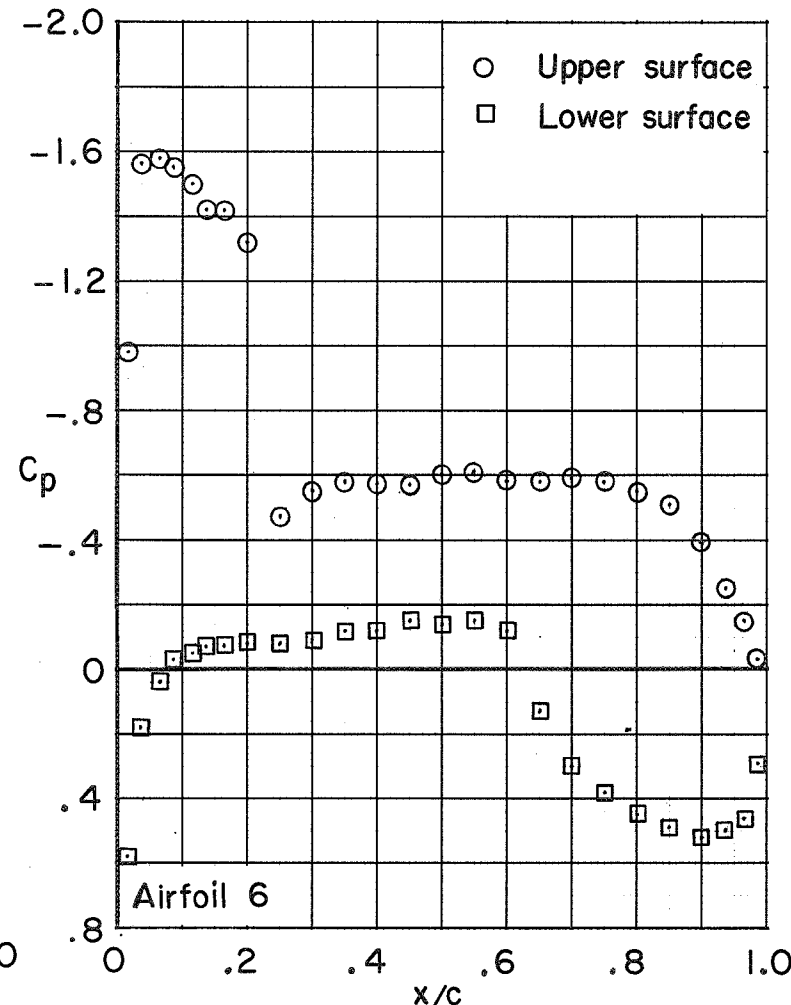
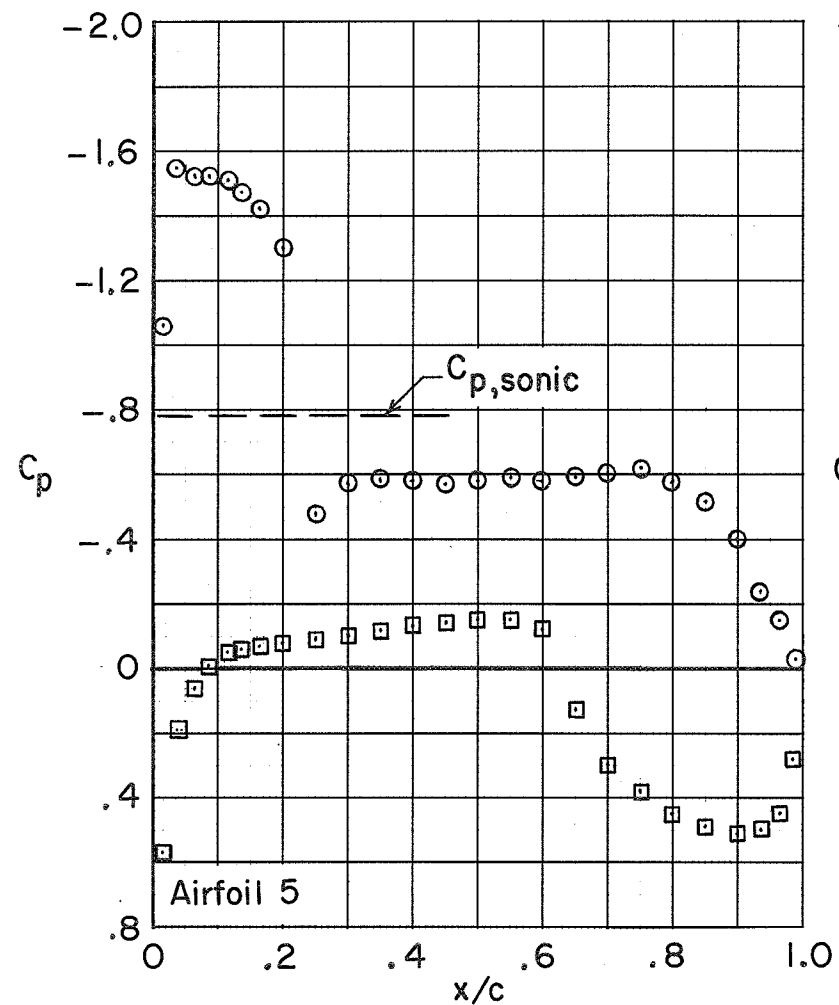
(f) $M = 0.70$; $\alpha = 1.5^\circ$.

Figure 7.- Continued.



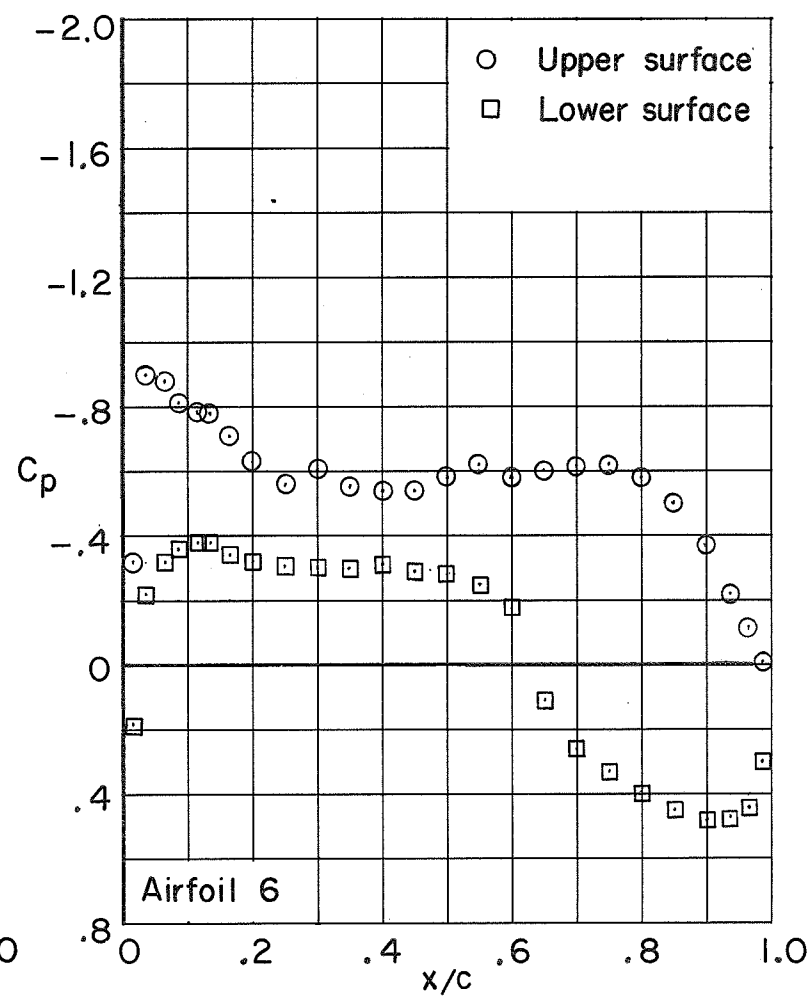
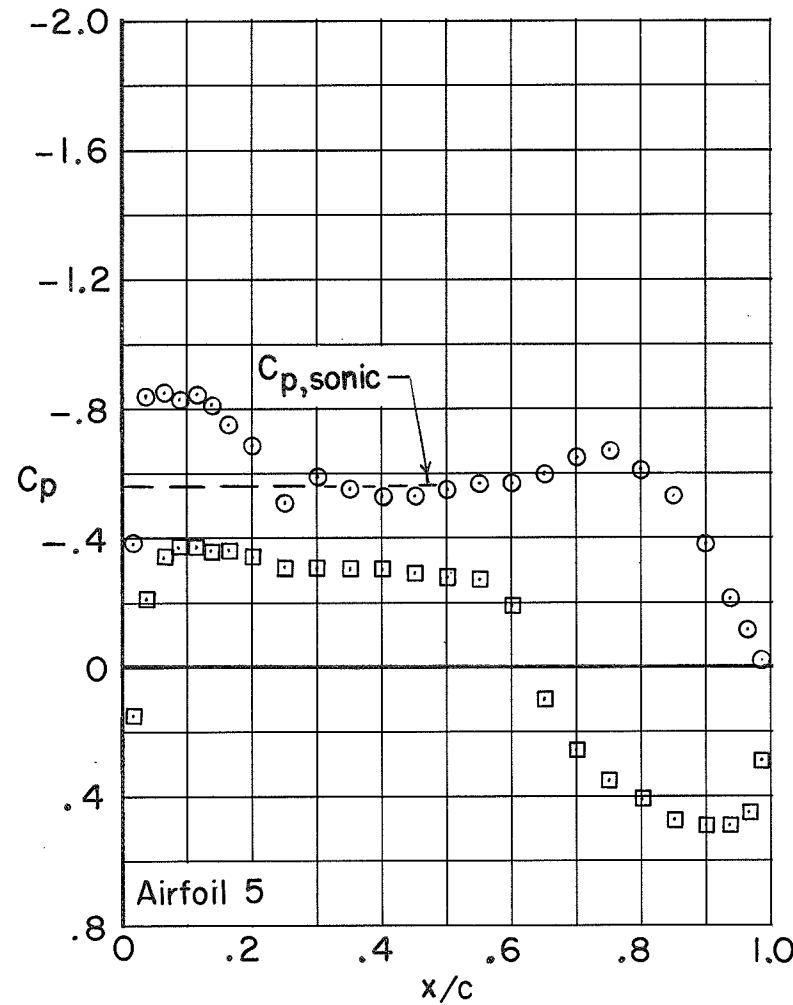
(g) $M = 0.70$; $\alpha = 2.0^\circ$.

Figure 7.- Continued.



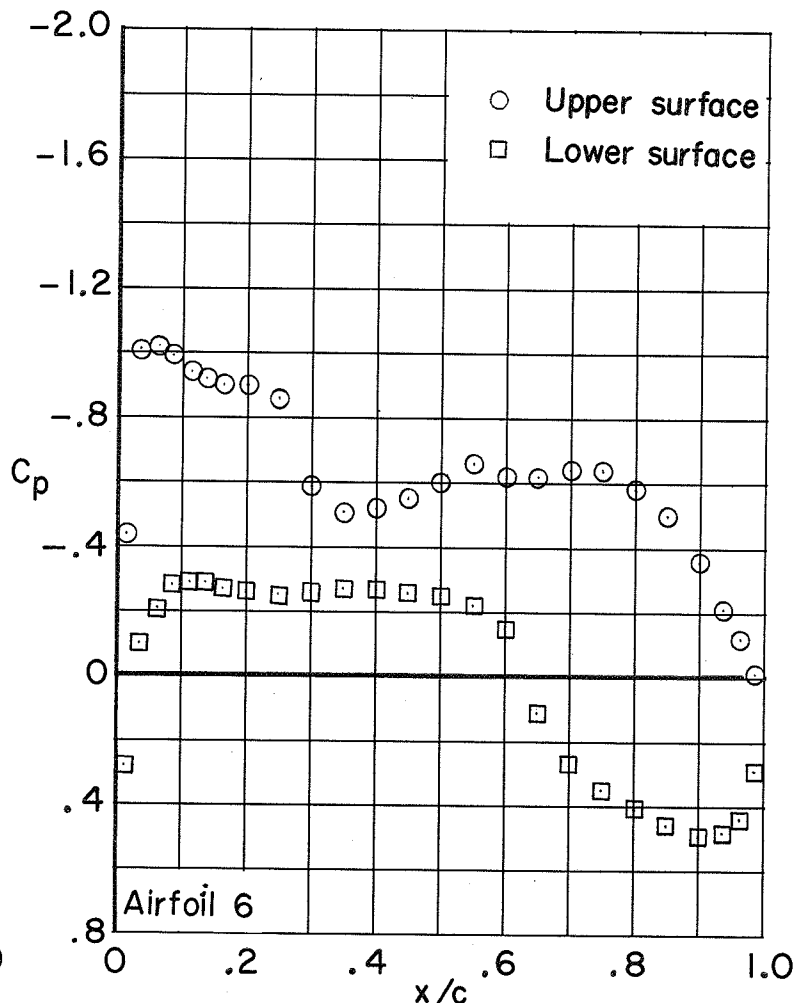
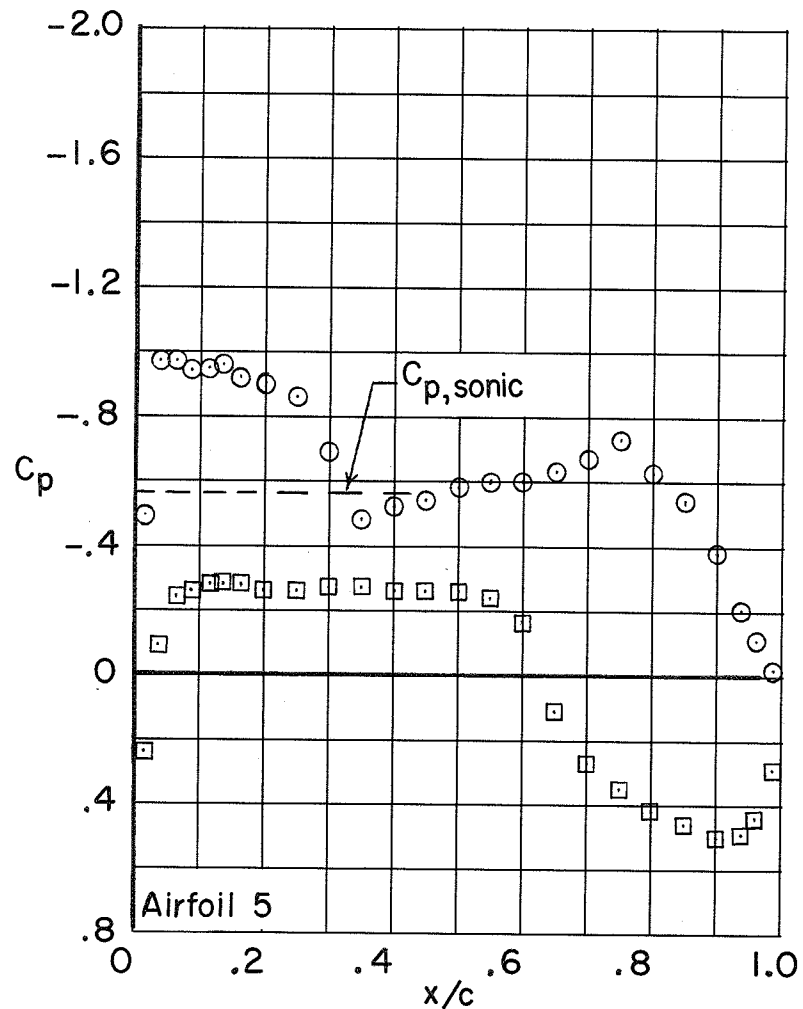
(h) $M = 0.70$; $\alpha = 2.5^\circ$.

Figure 7.- Continued.



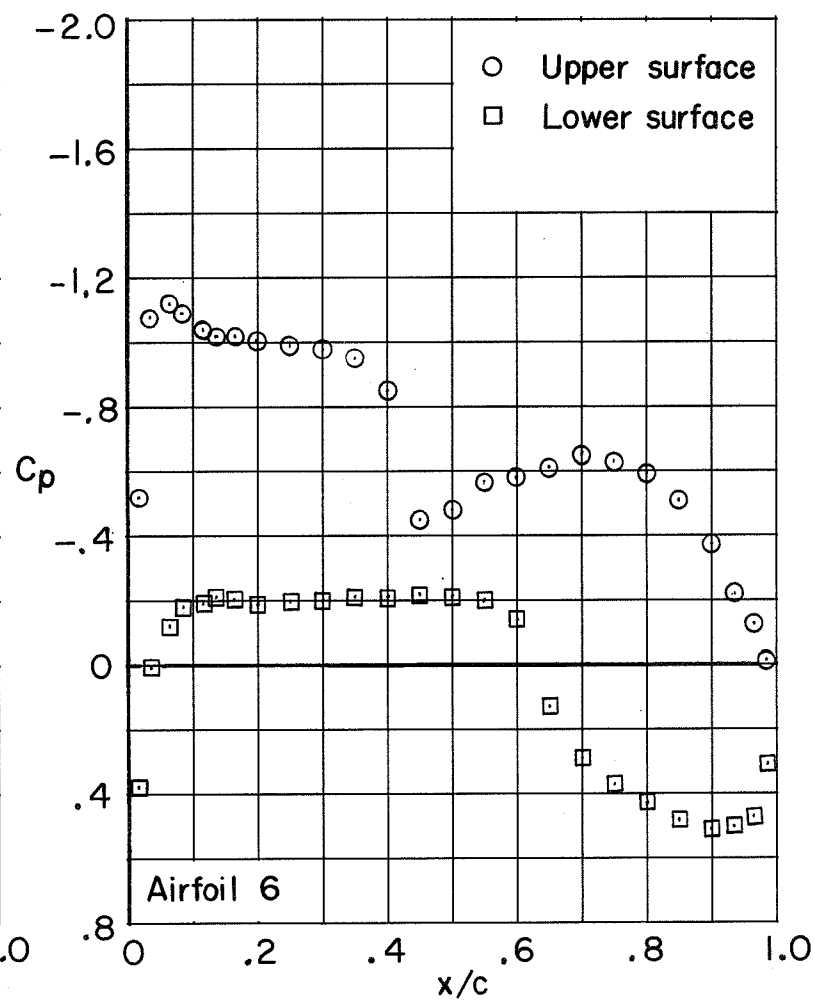
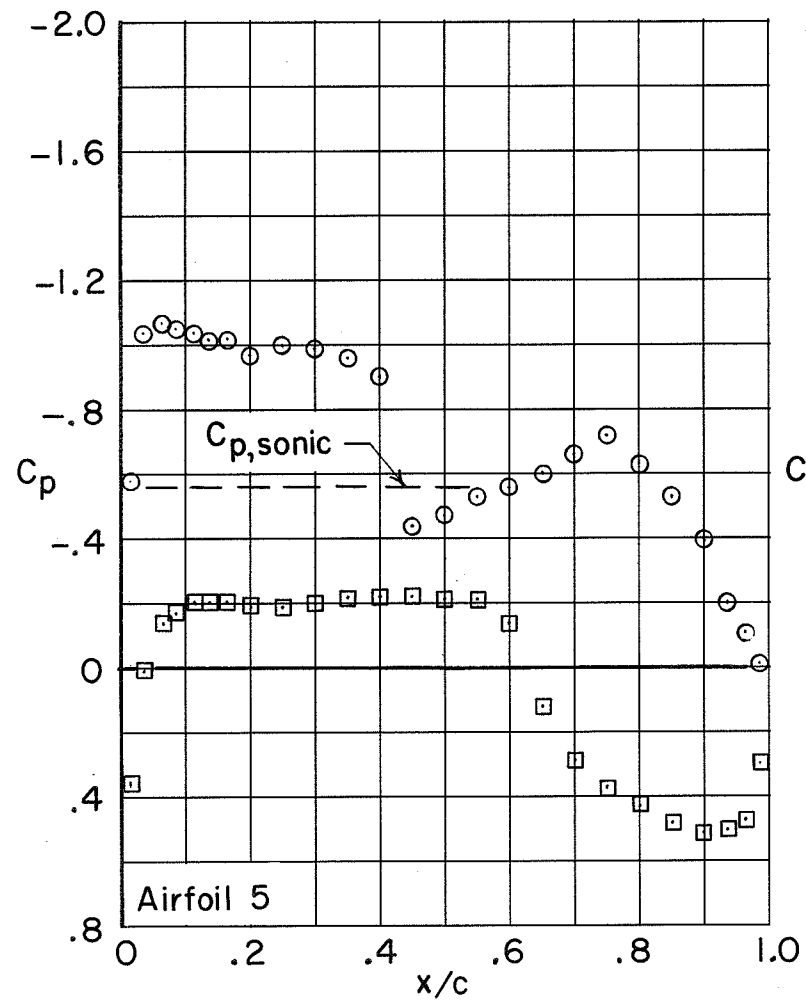
(i) $M = 0.76$; $\alpha = 0.5^\circ$.

Figure 7. - Continued.



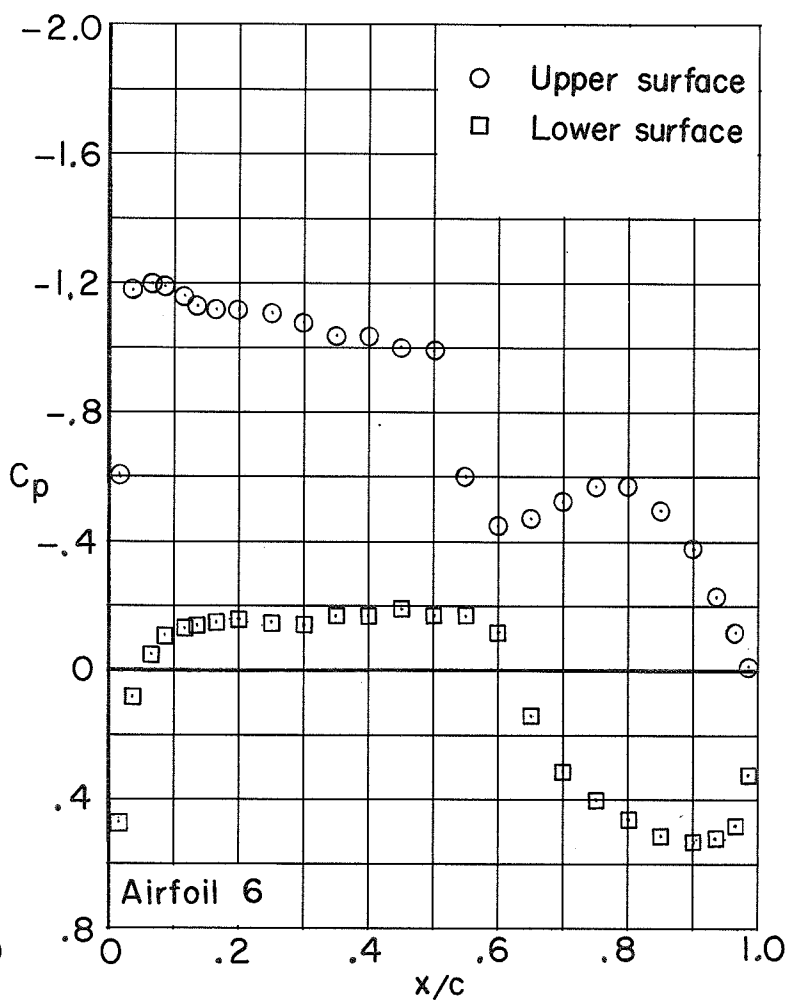
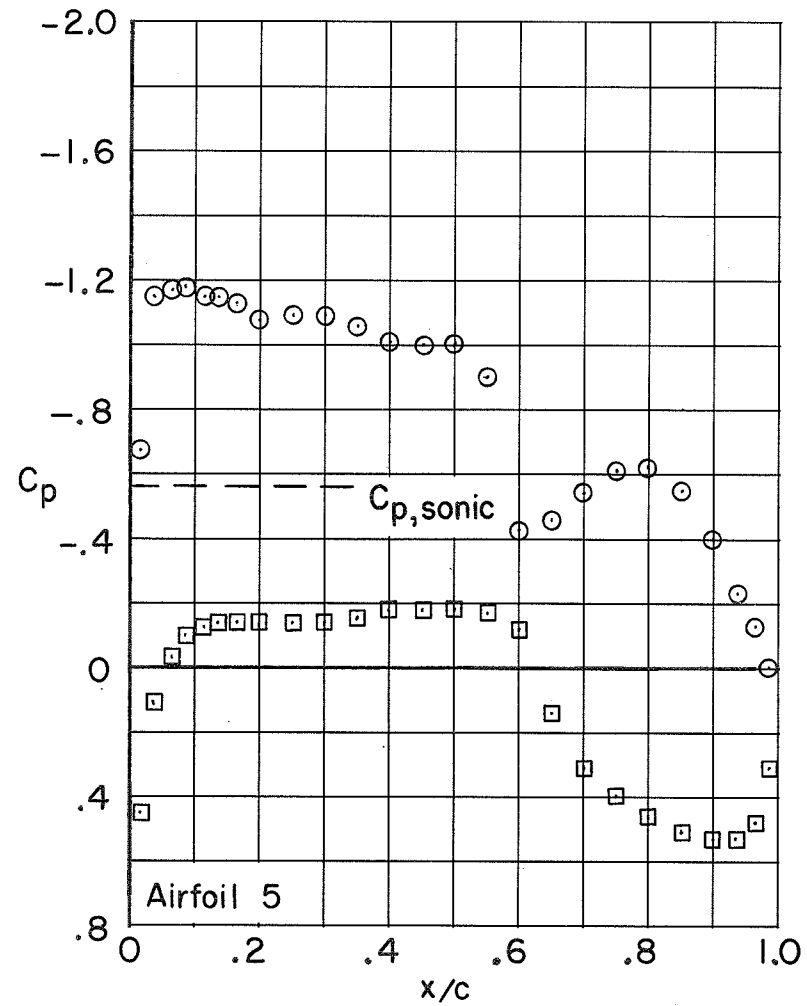
(j) $M = 0.76$; $\alpha = 1.0^\circ$.

Figure 7.- Continued.



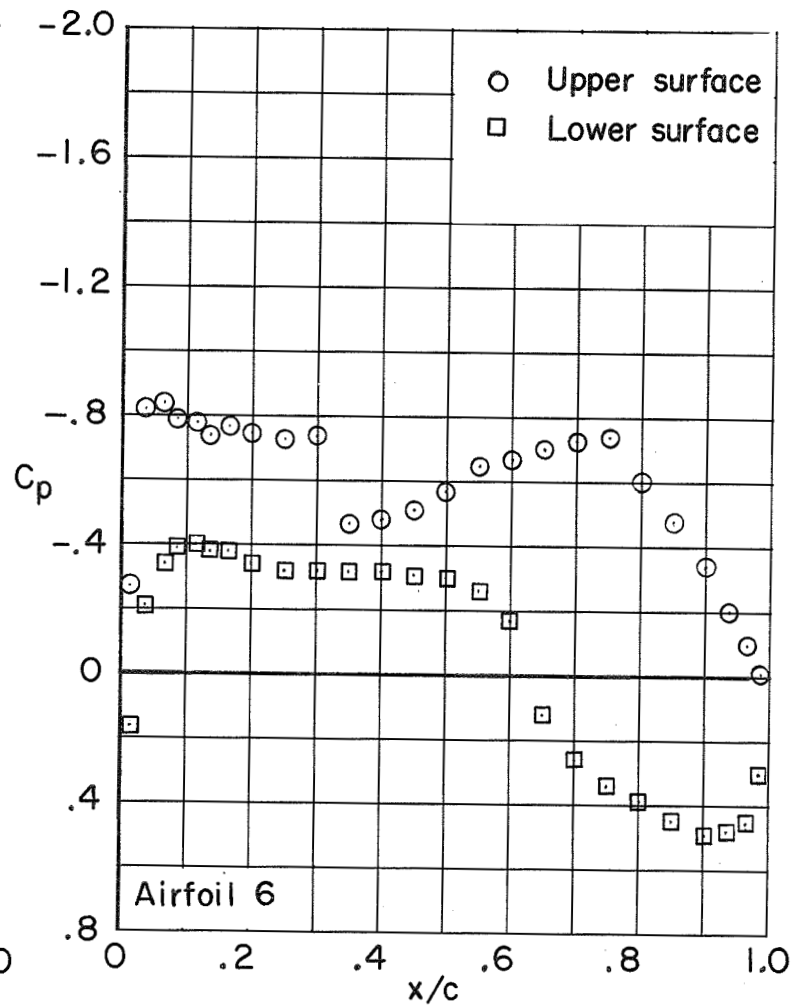
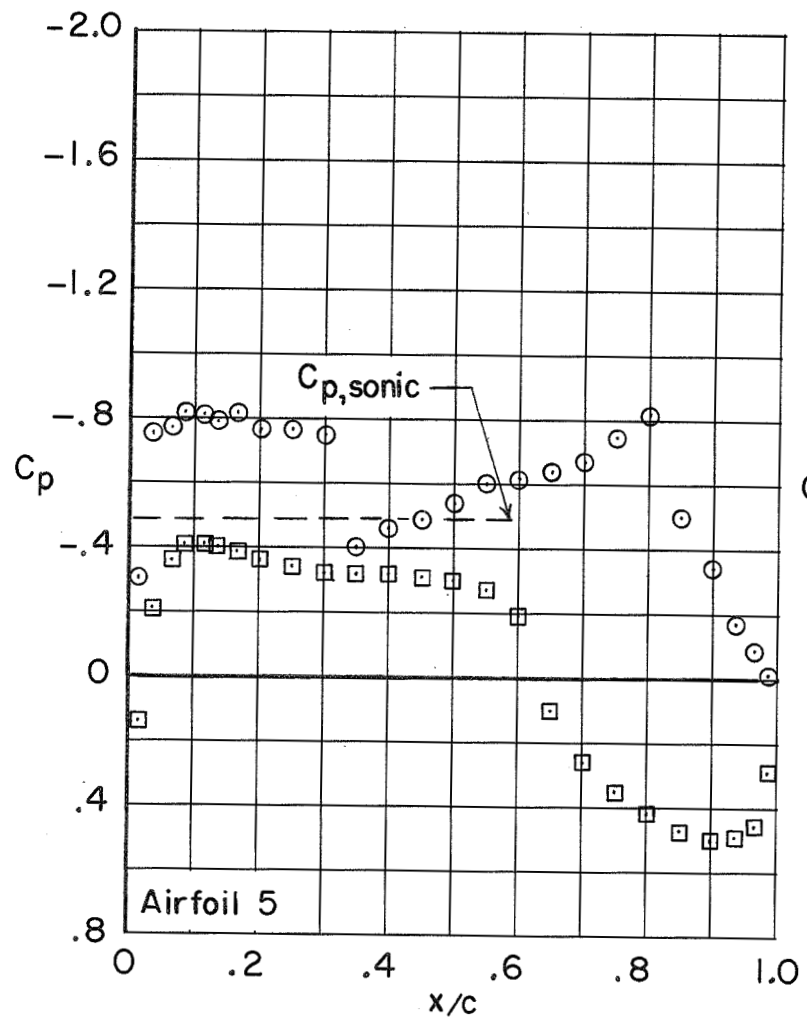
(k) $M = 0.76; \alpha = 1.5^\circ$.

Figure 7.- Continued.



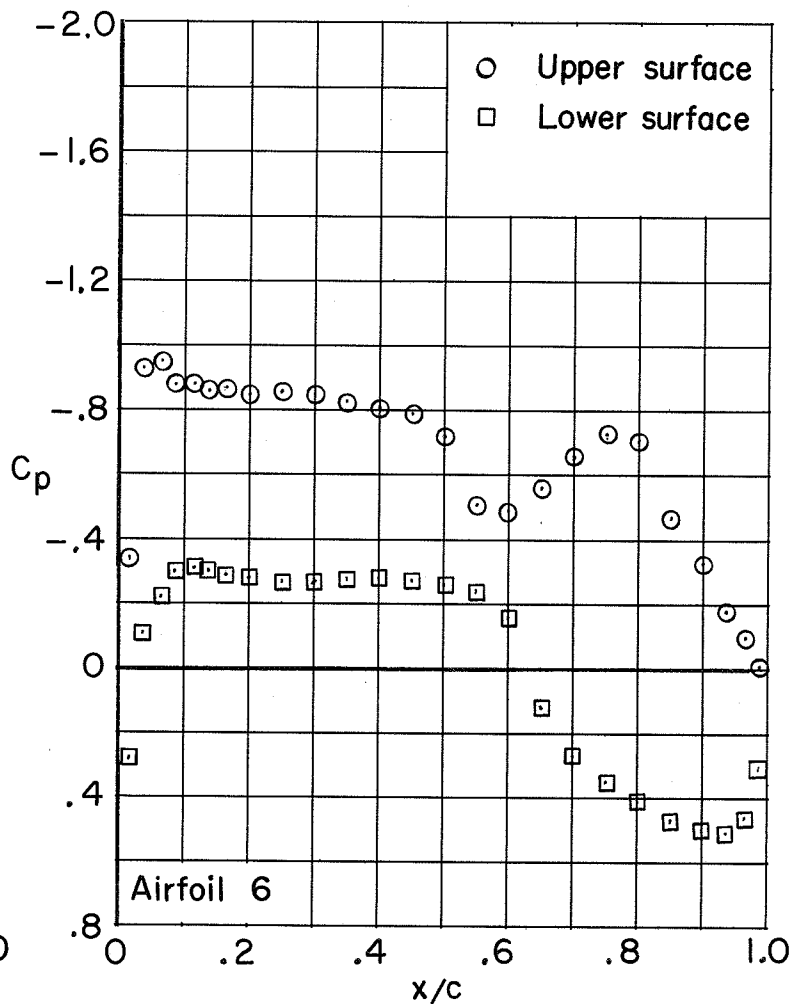
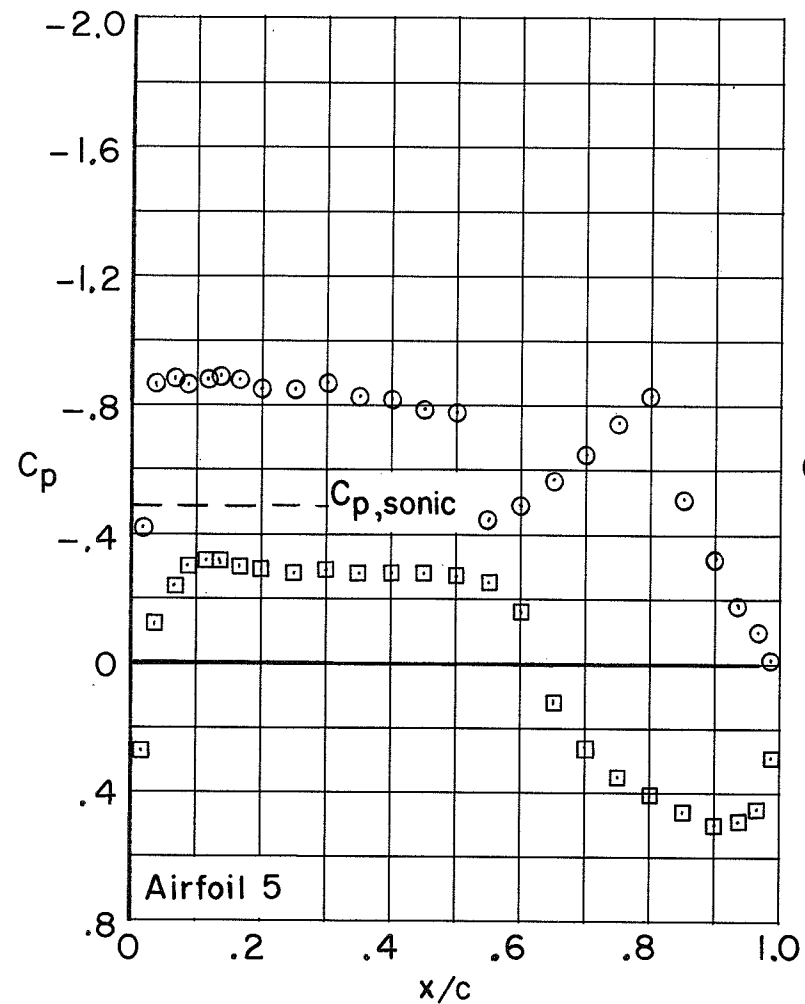
(1) $M = 0.76$; $\alpha = 2.0^\circ$.

Figure 7.- Continued.



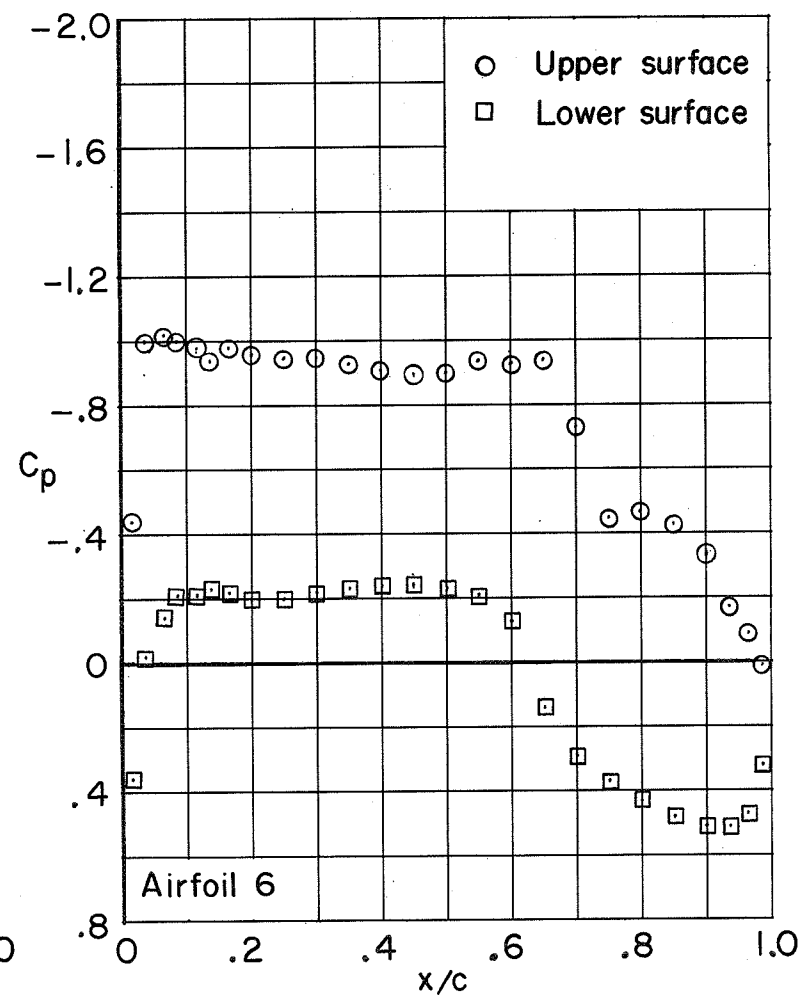
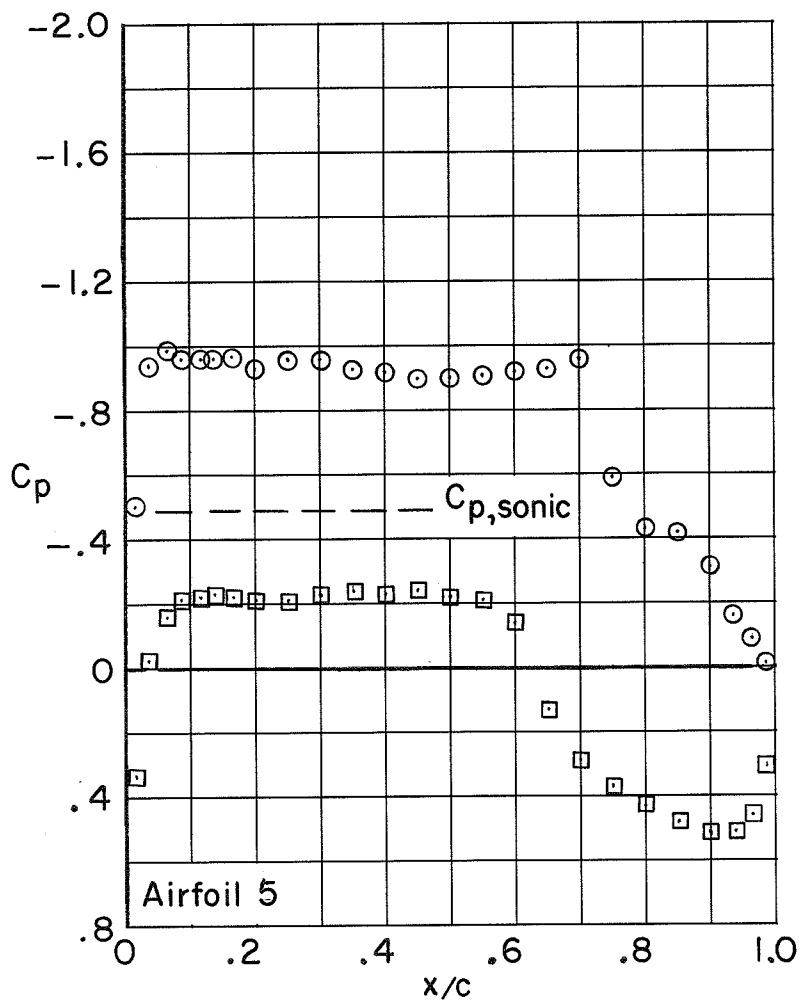
(m) $M = 0.78; \alpha = 0.5^\circ$.

Figure 7.- Continued.



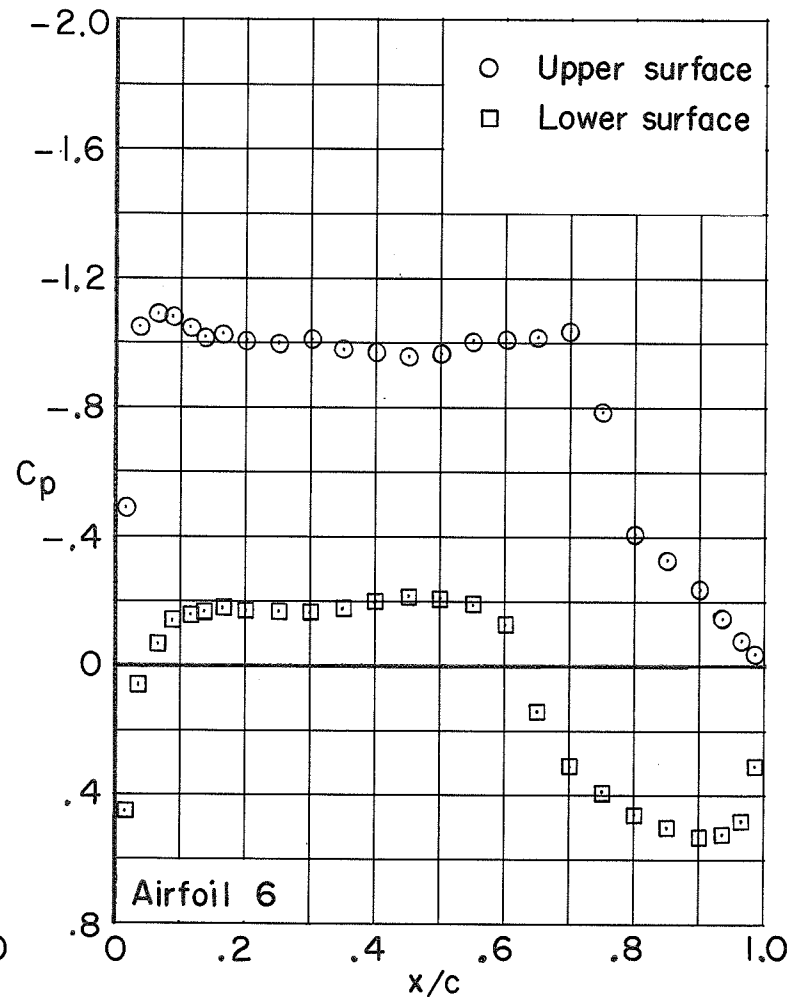
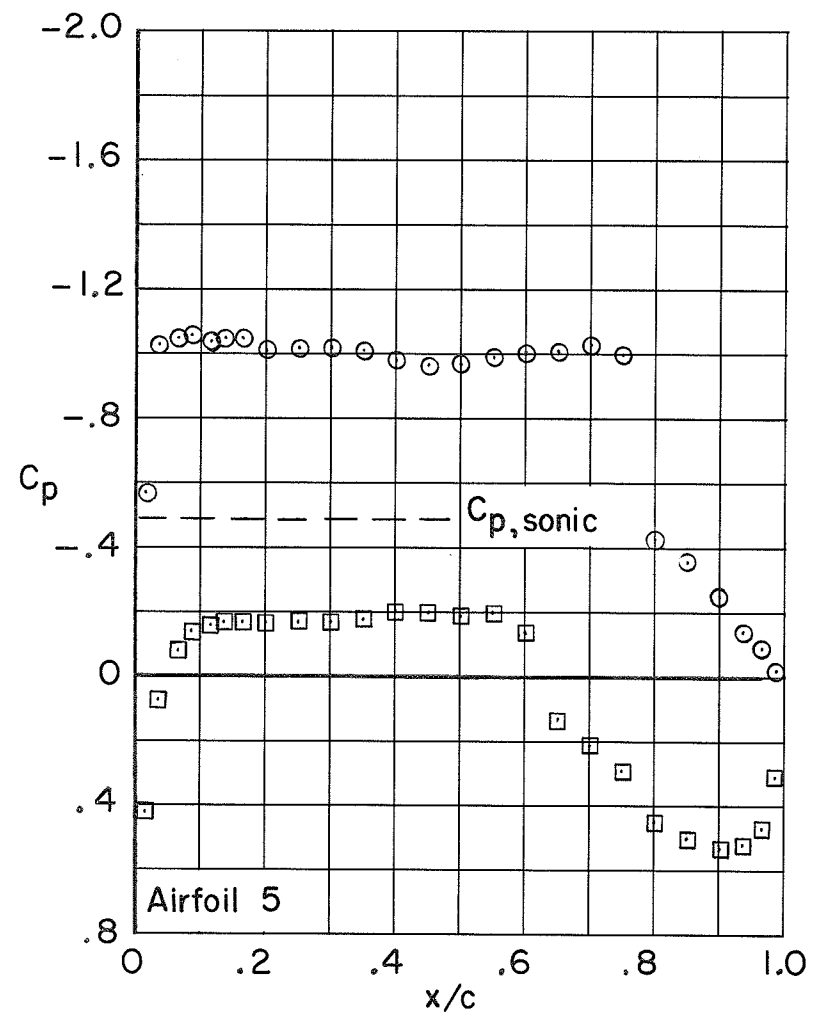
(n) $M = 0.78$; $\alpha = 1.0^\circ$.

Figure 7.- Continued.



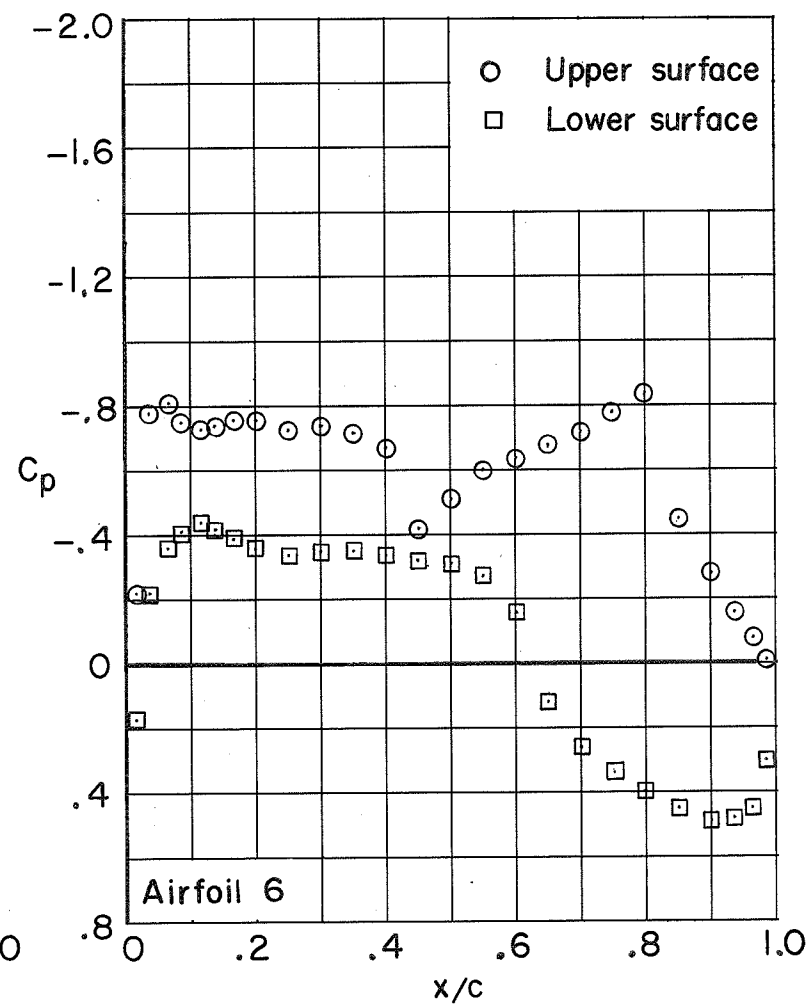
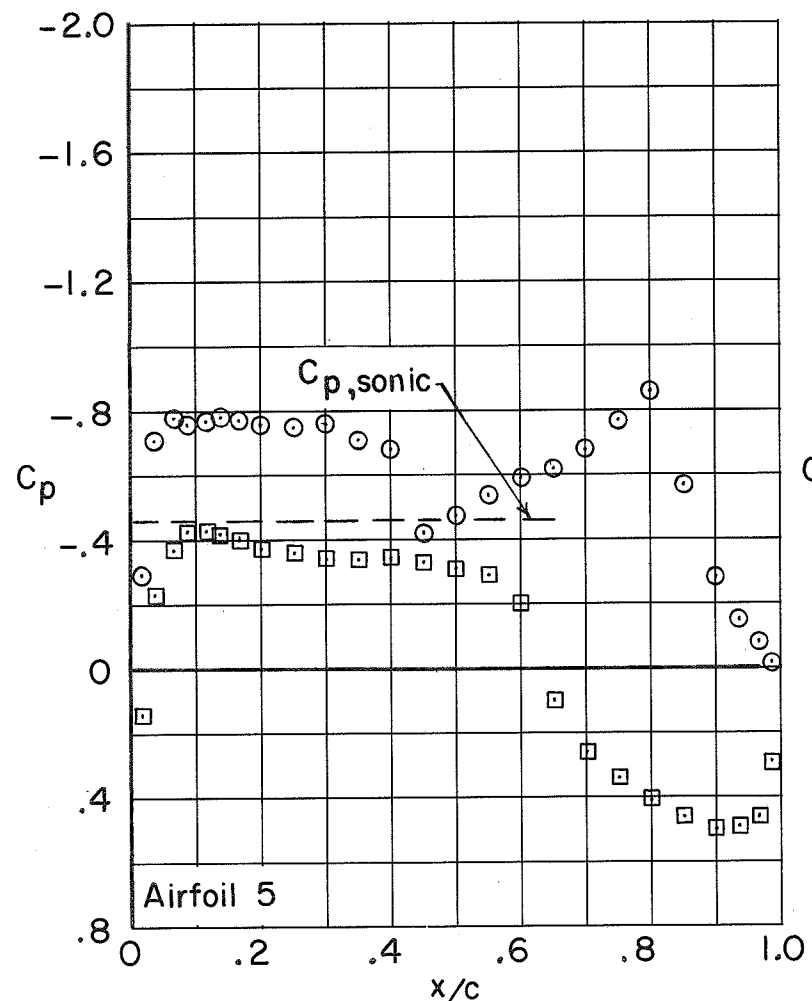
(o) $M = 0.78$; $\alpha = 1.5^\circ$.

Figure 7.- Continued.



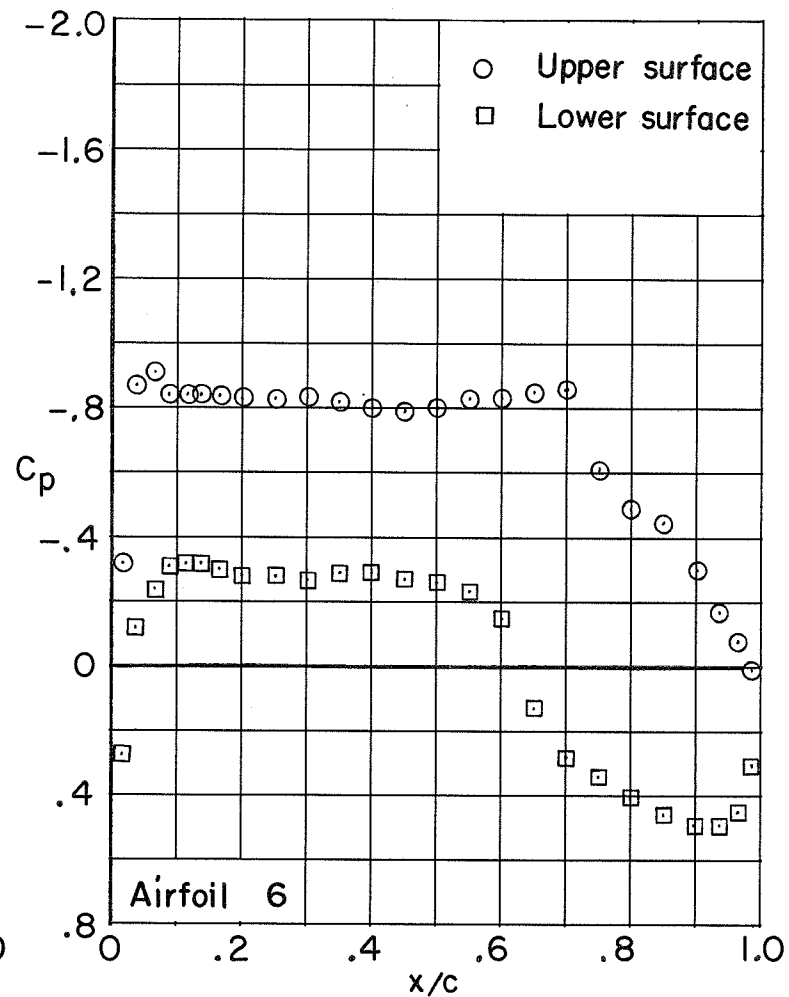
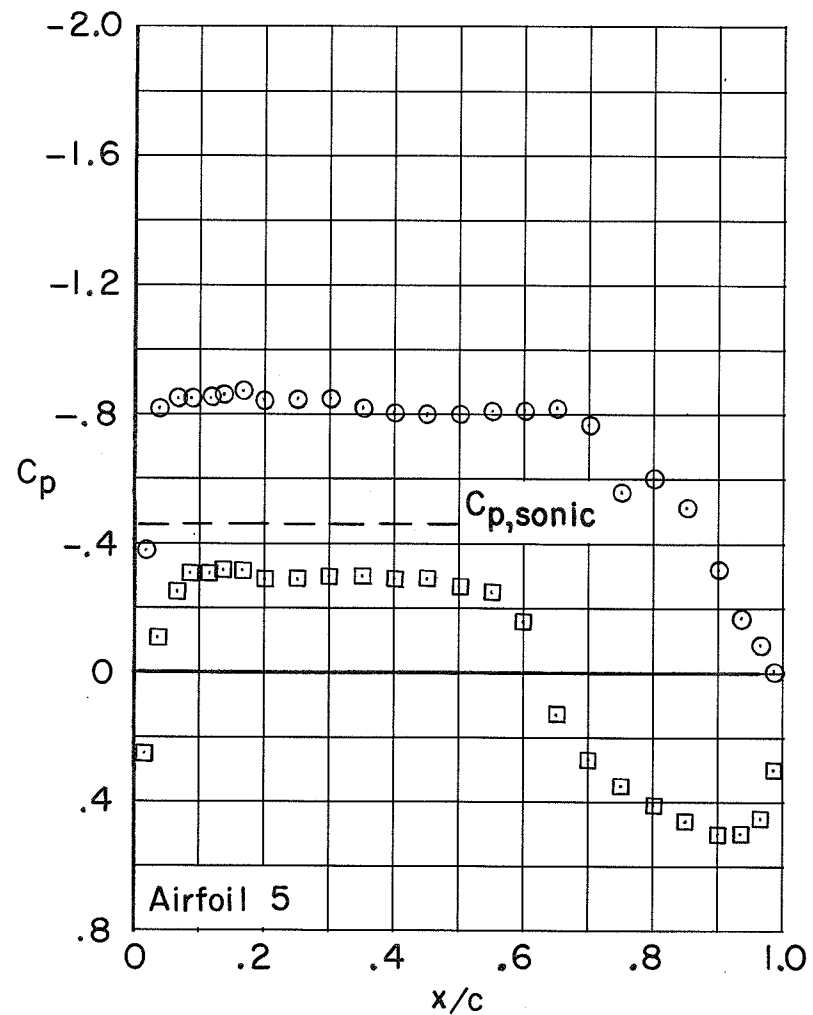
(p) $M = 0.78$; $\alpha = 2.0^\circ$.

Figure 7.- Continued.



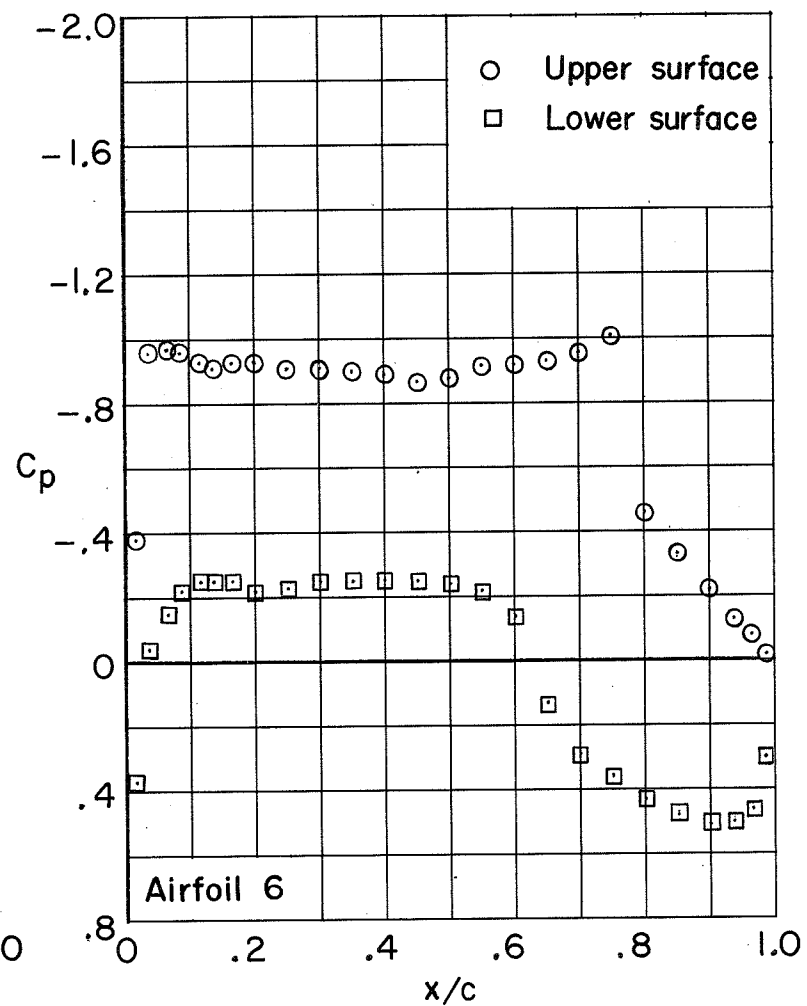
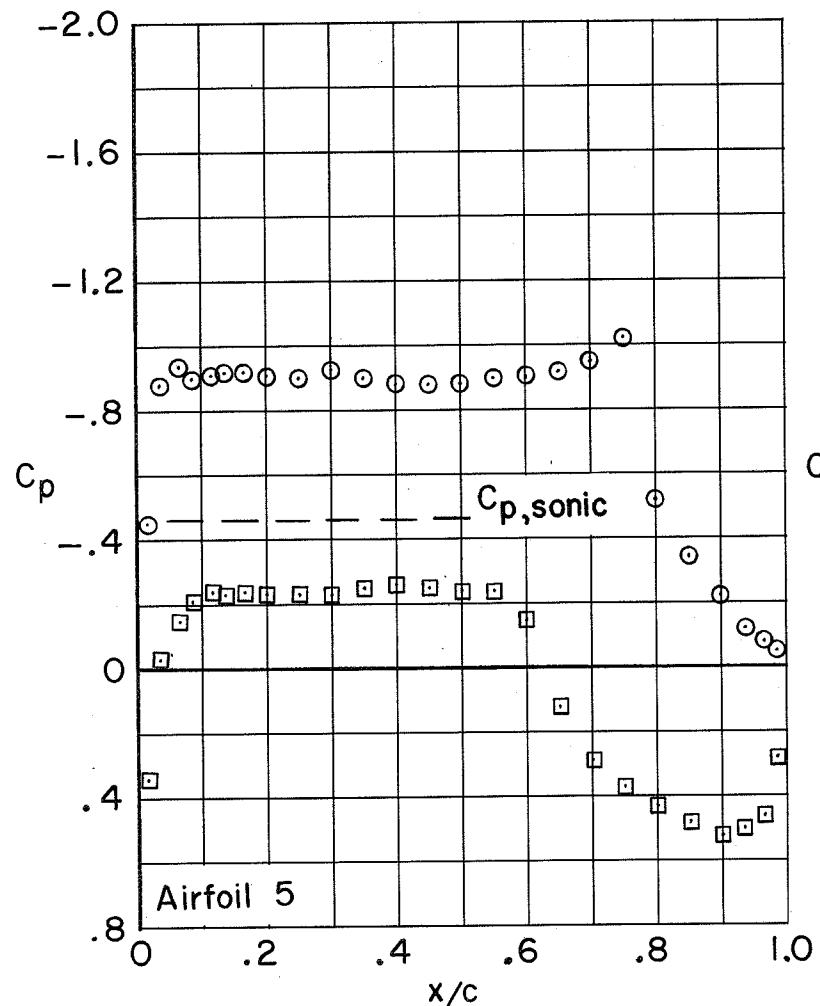
(q) $M = 0.79$; $\alpha = 0.5^\circ$.

Figure 7.- Continued.



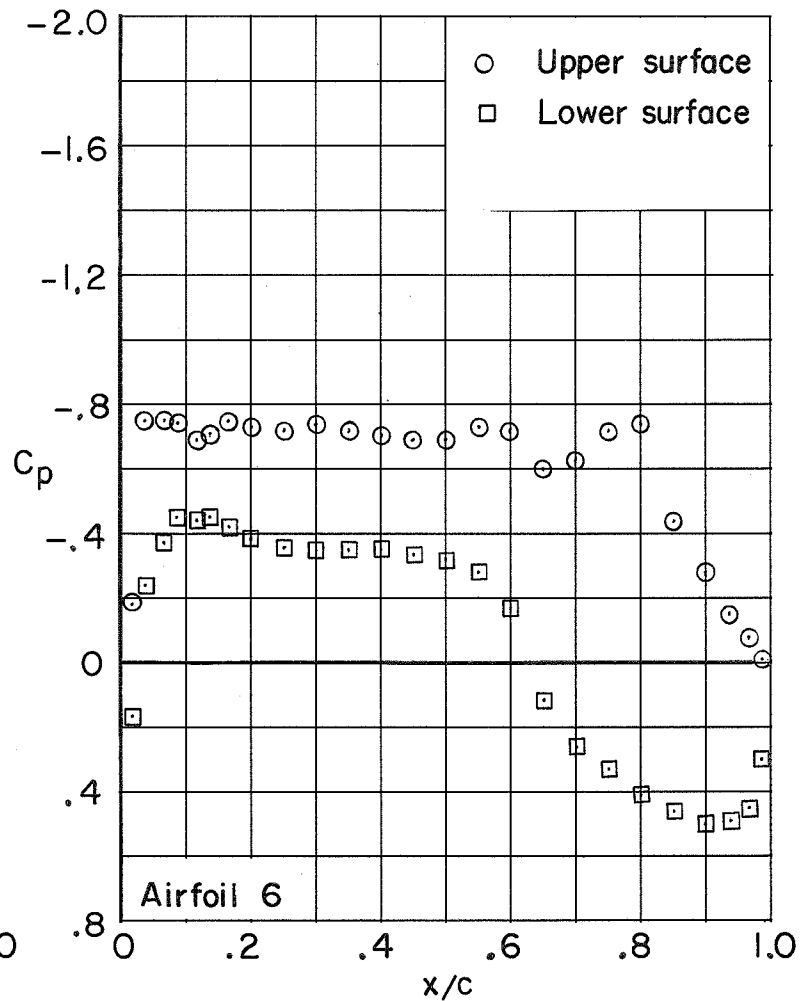
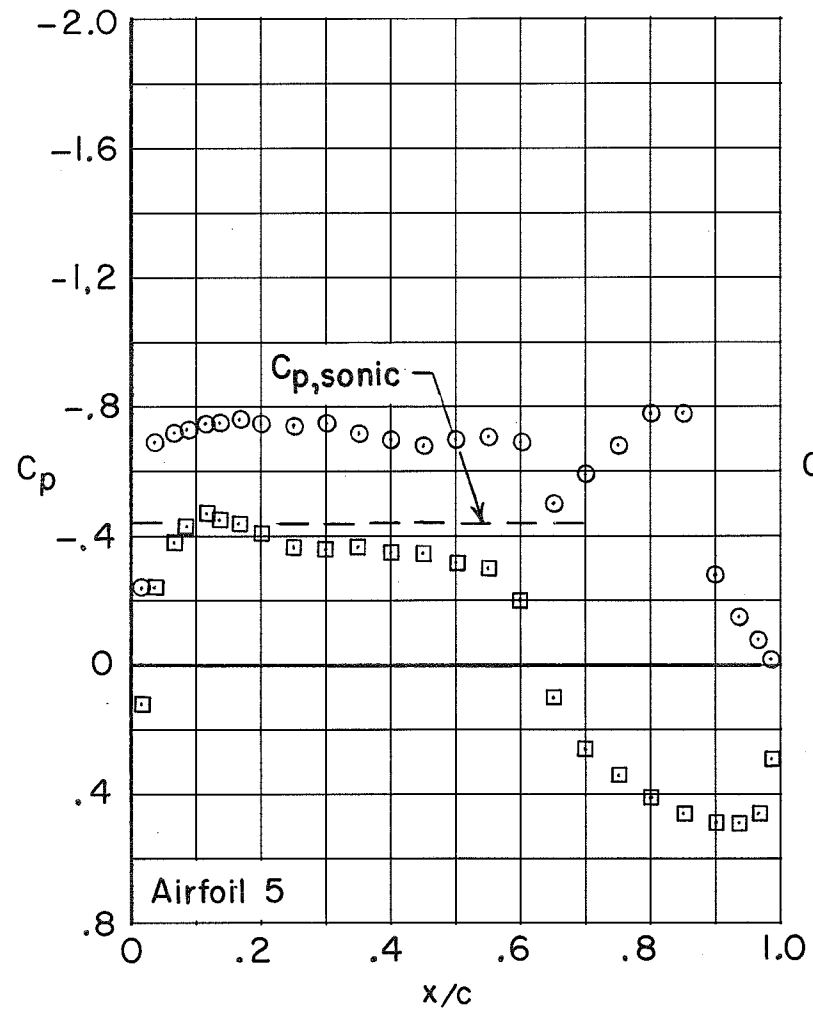
(r) $M = 0.79$; $\alpha = 1.0^\circ$.

Figure 7.- Continued.



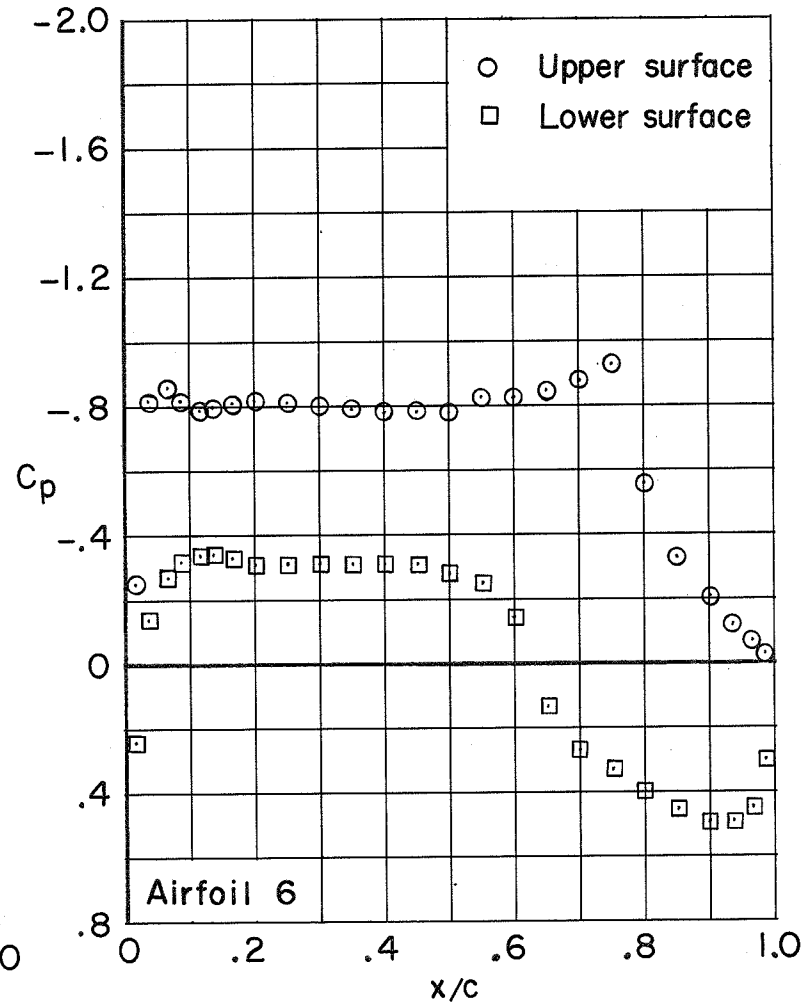
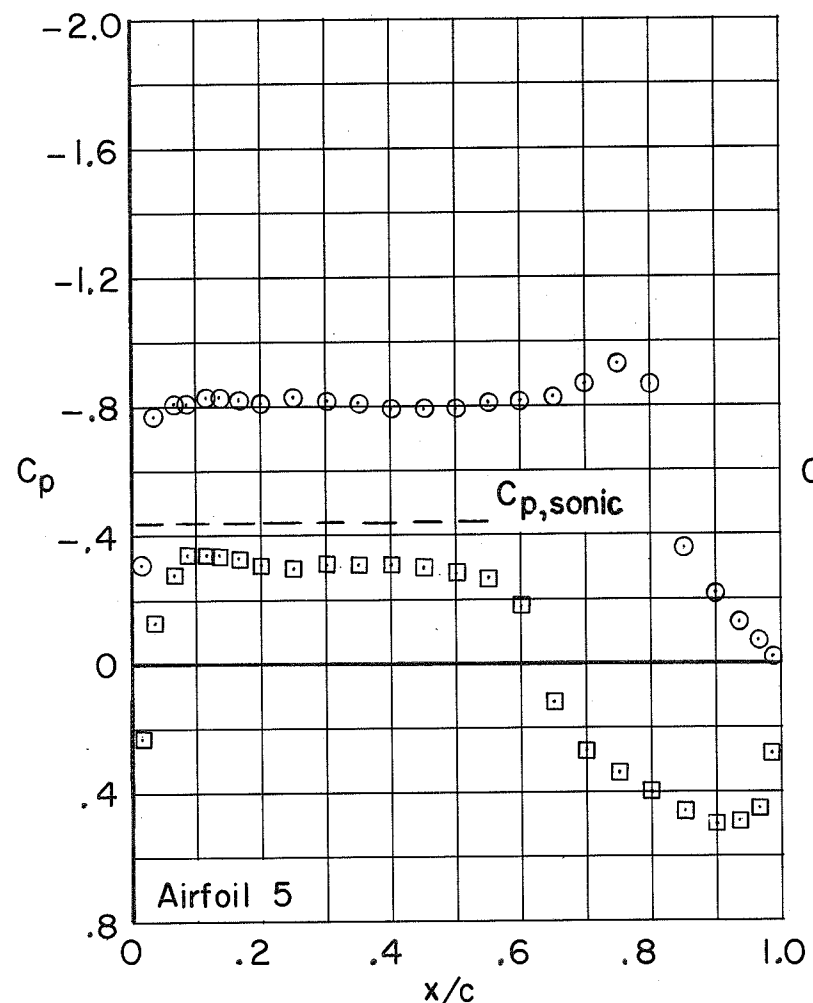
(s) $M = 0.79; \alpha = 1.5^\circ$.

Figure 7.- Continued.



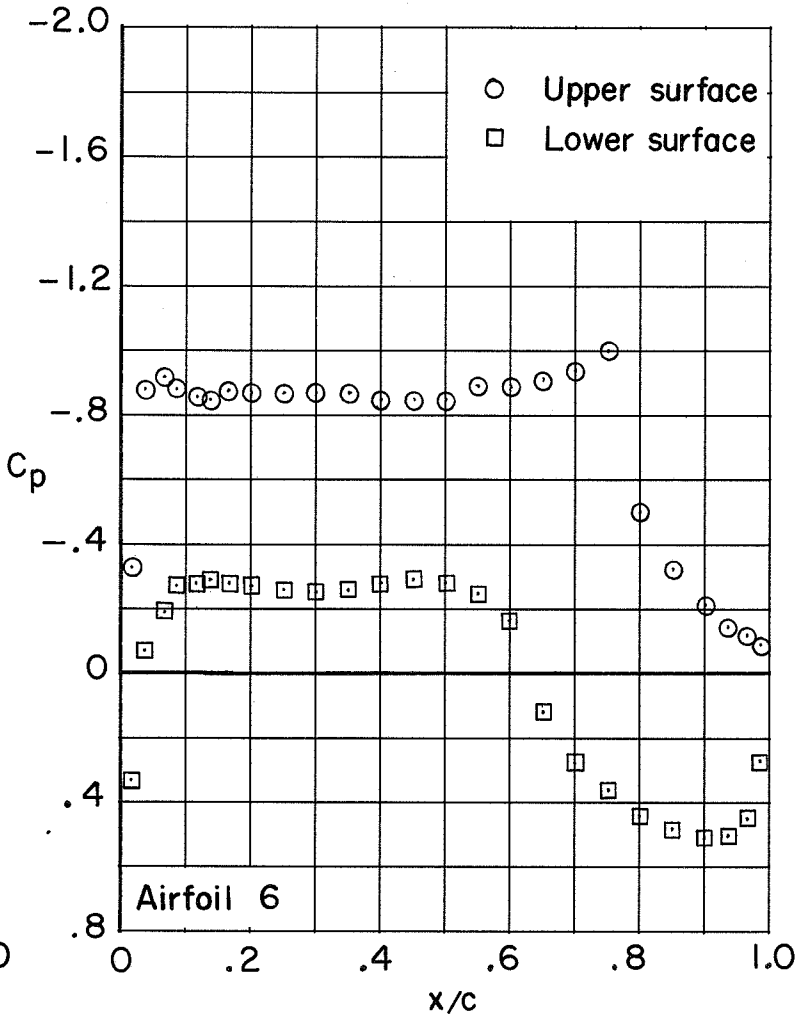
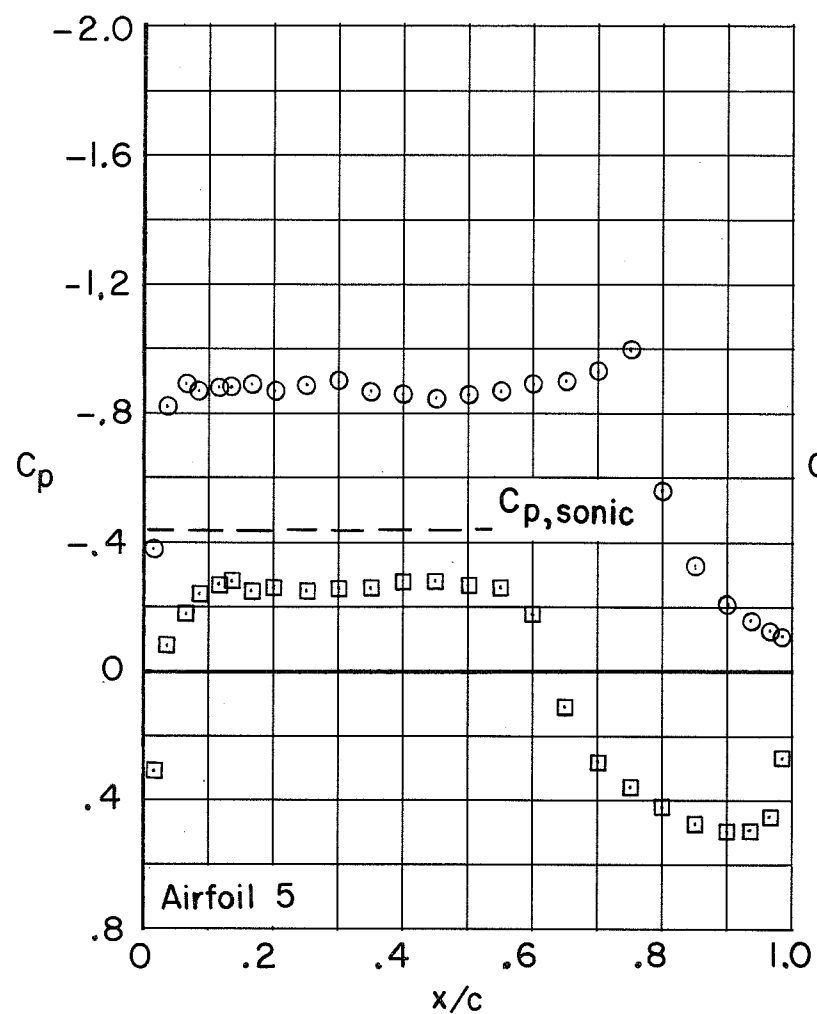
(t) $M = 0.80$; $\alpha = 0.5^0$.

Figure 7.- Continued.



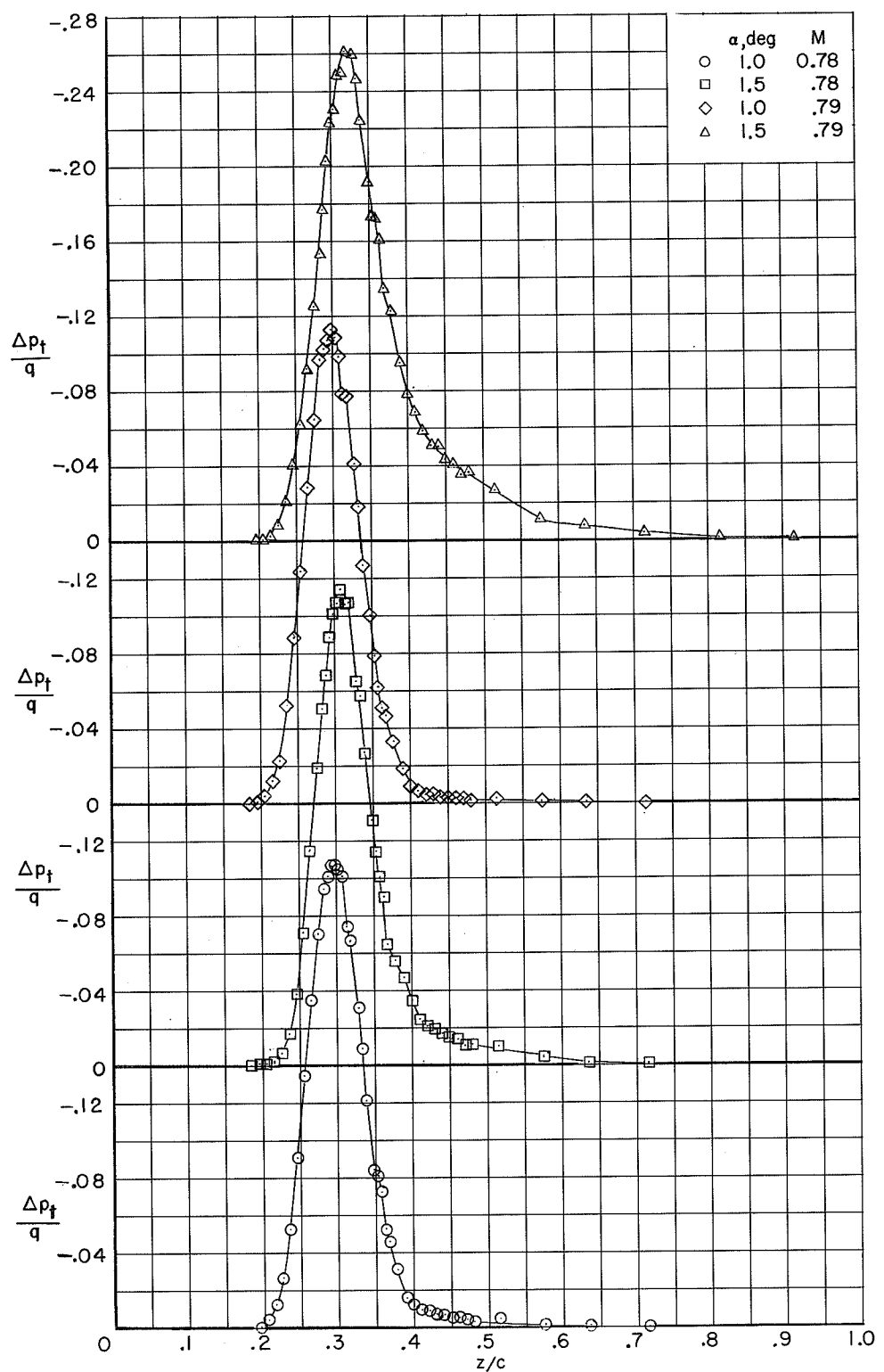
(u) $M = 0.80$; $\alpha = 1.0^\circ$.

Figure 7.- Continued.



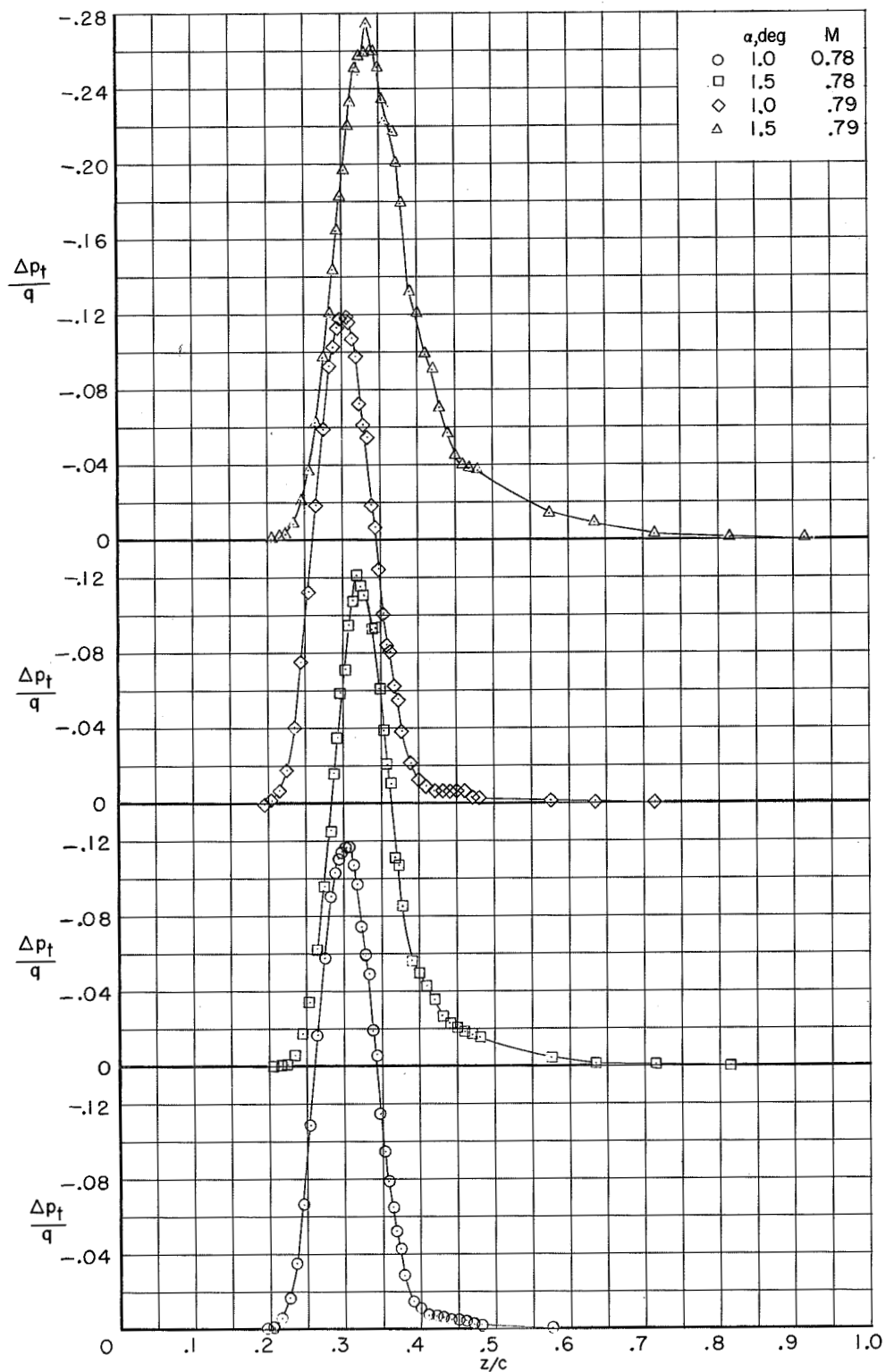
(v) $M = 0.80; \alpha = 1.5^0$.

Figure 7.- Concluded.



(a) Airfoil 5.

Figure 8.- Representative wake profiles.



(b) Airfoil 6.

Figure 8.- Concluded.

~~CONFIDENTIAL~~

~~CONFIDENTIAL~~

SCIENTIFIC AND TECHNICAL PUBLICATIONS

The development and dissemination of the latest scientific and technical information is a major responsibility of the Administration. The publication of these new findings of importance to the aerospace and space fields is a major contribution to the progress of science and technology in these fields and the welfare of man.

—NATIONAL AERONAUTICS AND SPACE ACT OF 1958

NASA SCIENTIFIC AND TECHNICAL PUBLICATIONS

TECHNICAL REPORTS. Scientific and technical information considered important, complex, and of long-term value to existing knowledge.

TECHNICAL NOTES. Information-based on specific knowledge of importance to a particular or unique knowledge.

TECHNICAL MEMORANDUM

Information concerning limited data and details of performance data, security classification, or other aspects.

CONFIRMATION REPORTS. Scientific and technical information generated under a NASA contract or grant and associated with certain confirmed scientific knowledge.

TECHNICAL TRANSLATIONS. Information published in a foreign language translated to English NASA distribution in English.

SPECIAL PUBLICATIONS. Information derived from one of value to NASA activities. Publications include conference proceedings, monographs, law compilations, handbooks, textbooks, and special bibliographies.

TECHNOLOGY TRANSLATIONS

PUBLIC AFFAIRS. Information on technology used by NASA that may be of particular interest to the general and other non-aerospace publics. Publications include Tech Briefs, Technology Utilization Reports and Notes, and Technology Surveys.

Details on the availability of these publications may be obtained from:

SCIENTIFIC AND TECHNICAL INFORMATION OFFICE

NATIONAL AERONAUTICS AND SPACE ADMINISTRATION

Washington, D.C. 20546

SCIENTIFIC AND TECHNICAL PUBLICATIONS